NSRDS—NBS 41

NATIONAL STANDARD NSRDS REFERENCE DATA SYSTEM

Crystal Structure Transformations in Binary Halides

U.S. DEPARTMENT OF COMMERCE
National Bureau of Standards

NATIONAL BUREAU OF STANDARDS

The National Bureau of Standards[1] was established by an act of Congress March 3, 1901. The Bureau's overall goal is to strengthen and advance the Nation's science and technology and facilitate their effective application for public benefit. To this end, the Bureau conducts research and provides: (1) a basis for the Nation's physical measurement system, (2) scientific and technological services for industry and government, (3) a technical basis for equity in trade, and (4) technical services to promote public safety. The Bureau consists of the Institute for Basic Standards, the Institute for Materials Research, the Institute for Applied Technology, the Center for Computer Sciences and Technology, and the Office for Information Programs.

THE INSTITUTE FOR BASIC STANDARDS provides the central basis within the United States of a complete and consistent system of physical measurement; coordinates that system with measurement systems of other nations; and furnishes essential services leading to accurate and uniform physical measurements throughout the Nation's scientific community, industry, and commerce. The Institute consists of a Center for Radiation Research, an Office of Measurement Services and the following divisions:

Applied Mathematics—Electricity—Heat—Mechanics—Optical Physics—Linac Radiation[2]—Nuclear Radiation[2]—Applied Radiation[2]—Quantum Electronics[3]—Electromagnetics—Time and Frequency[3]—Laboratory Astrophysics[3]—Cryogenics[3].

THE INSTITUTE FOR MATERIALS RESEARCH conducts materials research leading to improved methods of measurement, standards, and data on the properties of well-characterized materials needed by industry, commerce, educational institutions, and Government; provides advisory and research services to other Government agencies; and develops, produces, and distributes standard reference materials. The Institute consists of the Office of Standard Reference Materials and the following divisions:

Analytical Chemistry—Polymers—Metallurgy—Inorganic Materials—Reactor Radiation—Physical Chemistry.

THE INSTITUTE FOR APPLIED TECHNOLOGY provides technical services to promote the use of available technology and to facilitate technological innovation in industry and Government; cooperates with public and private organizations leading to the development of technological standards (including mandatory safety standards), codes and methods of test; and provides technical advice and services to Government agencies upon request. The Institute also monitors NBS engineering standards activities and provides liaison between NBS and national and international engineering standards bodies. The Institute consists of the following divisions and offices:

Engineering Standards Services—Weights and Measures—Invention and Innovation—Product Evaluation Technology—Building Research—Electronic Technology—Technical Analysis—Measurement Engineering—Office of Fire Programs.

THE CENTER FOR COMPUTER SCIENCES AND TECHNOLOGY conducts research and provides technical services designed to aid Government agencies in improving cost effectiveness in the conduct of their programs through the selection, acquisition, and effective utilization of automatic data processing equipment; and serves as the principal focus within the executive branch for the development of Federal standards for automatic data processing equipment, techniques, and computer languages. The Center consists of the following offices and divisions:

Information Processing Standards—Computer Information—Computer Services—Systems Development—Information Processing Technology.

THE OFFICE FOR INFORMATION PROGRAMS promotes optimum dissemination and accessibility of scientific information generated within NBS and other agencies of the Federal Government; promotes the development of the National Standard Reference Data System and a system of information analysis centers dealing with the broader aspects of the National Measurement System; provides appropriate services to ensure that the NBS staff has optimum accessibility to the scientific information of the world, and directs the public information activities of the Bureau. The Office consists of the following organizational units:

Office of Standard Reference Data—Office of Technical Information and Publications—Library—Office of International Relations.

[1] Headquarters and Laboratories at Gaithersburg, Maryland, unless otherwise noted; mailing address Washington, D.C. 20234.
[2] Part of the Center for Radiation Research.
[3] Located at Boulder, Colorado 80302.

UNITED STATES DEPARTMENT OF COMMERCE • PETER G. PETERSON, *Secretary*

U. S. NATIONAL BUREAU OF STANDARDS • LAWRENCE M. RUSHNER, *Acting Director*

Crystal Structure Transformations in Binary Halides

C. N. R. Rao and M. Natarajan

Department of Chemistry
Indian Institute of Technology
Kanpur-16, India

NSRDS-NBS 41

Nat. Stand. Ref. Data Ser., Nat. Bur. Stand. (U.S.), 41, 53 pages (July 1972)
CODEN: NSRDAP

Issued July 1972

For sale by the Superintendent of Documents, U.S. Government Printing Office
Washington, D.C., 20402 (Order by SD Catalog No. C 13.48:41)-Price 55 cents
Stock Number 0303-0964

Library of Congress Catalog Card Number: 78-186213

Foreword

The National Standard Reference Data System provides access to the quantitative data of physical science, critically evaluated and compiled for convenience, and readily accessible through a variety of distribution channels. The System was established in 1963 by action of the President's Office of Science and Technology and the Federal Council for Science and Technology, with responsibility to administer it assigned to the National Bureau of Standards.

The System now comprises a complex of data centers and other activities, carried on in academic institutions and other laboratories both in and out of government. The independent operational status of existing critical data projects is maintained and encouraged. Data centers that are components of the NSRDS produce compilations of critically evaluated data, critical reviews of the state of quantitative knowledge in specialized areas, and computations of useful functions derived from standard reference data. In addition, the centers and projects establish criteria for evaluation and compilation of data and make recommendations on needed improvements in experimental techniques. They are normally closely associated with active research in the relevant field.

The technical scope of the NSRDS is indicated by the principal categories of data compilation projects now active or being planned: nuclear properties, atomic and molecular properties, solid state properties, thermodynamic and transport properties, chemical kinetics, and colloid and surface properties.

The NSRDS receives advice and planning assistance from the National Research Council of the National Academy of Sciences-National Academy of Engineering. An overall Review Committee considers the program as a whole and makes recommendations on policy, long-term planning, and international collaboration. Advisory Panels, each concerned with a single technical area, meet regularly to examine major portions of the program, assign relative priorities, and identify specific key problems in need of further attention. For selected specific topics, the Advisory Panels sponsor subpanels which make detailed studies of users' needs, the present state of knowledge, and existing data resources as a basis for recommending one or more data compilation activities. This assembly of advisory services contributes greatly to the guidance of NSRDS activities.

The NSRDS–NBS series of publications is intended primarily to include evaluated reference data and critical reviews of long-term interest to the scientific and technical community.

Lawrence M. Kushner, *Acting Director*

Preface

Many solids undergo transformations from one crystal structure to another. Studies of such phase transformations are of great value in understanding the nature and properties of solid materials. Recent literature abounds in information on the phase transformations of solids and it is often difficult to obtain relevant data or references on the transformations of any specific solid. We, therefore, considered it worthwhile to collect the literature on the phase transformations of various types of inorganic solids and present them in an organized manner.

In this and subsequent reviews are summarized the important data and conclusions regarding the crystal structure transformations of a few series of inorganic solids. In doing so, we have surveyed most of the material abstracted up to 1970 in Chemical Abstracts and Solid State Abstracts. We have, however, not listed references to the entire published literature on the transformations of a given solid, but have presented only the crucial ones. We believe that all the literature can be traced back through the references listed at the end of each section. In reporting the data on the transformations of a solid we have indicated the methods employed as well as the important data and conclusions from the study. For each solid we have given the crystal structure data for the stable phase around room temperature and at atmospheric pressure making use of the standard patterns of the NBS and ACA Crystal Data; we have indicated the temperature wherever data are available.

The crystal structure transformations of binary halides form the subject matter of this review. This will be followed by reviews on the transformations of binary oxides and other systems.

Contents

Crystal Structure Transformations in Binary Halides*

C. N. R. Rao and M. Natarajan

A critical survey of the data describing crystal structure transformations in binary halides is compiled. Data on thermodynamic, crystallographic, spectroscopic and electronic properties are given for each transformation. Experimental techniques used to obtain the data are named and comments on the data are included in the tables. The literature is surveyed up to 1970. References have been selected on the basis of their pertinence to the data which are cited and do not represent all the available literature.

Key words: Binary halides; crystal structure transformation; electronic data; phase transformation; spectroscopic data; thermodynamic data; x-ray diffraction data.

Symbols Employed

P = Pressure
T = Temperature in K
T_t = Transformation temperature
ΔT = Thermal hysteresis in a reversible transformation
P_T = Transformation pressure
ΔH_{tr} = Enthalpy change accompanying the transformation
C_p = Heat capacity at constant pressure
ΔS = Entropy change
ΔV = Change in volume accompanying a transition
ρ = Density
α = Volume thermal expansion coefficient
η = Linear thermal expansion coefficient
ϵ = Dielectric constant
P_s = Spontaneous polarization
E_c = Coercive field
tan δ = Dissipation factor
σ = Electrical conductivity
E_a = Energy of activation
E_c^m = Cation migration energy
E_s = Formation energy of Schottky defects
atm = Atmosphere
cal = Calorie
eV = Electron volt
DTA = Differential thermal analysis
IR = Infrared
Z = Number of molecules per unit cell
NMR = Nuclear magnetic resonance
NQR = Nuclear quadrupole resonance
EPR = Electron paramagnetic resonance

Introduction

There has been increasing activity in recent years in the area of crystal structure transformations in inorganic solids. A variety of experimental techniques has been employed to study these phase transformations. Valuable information has been obtained on the crystallography, thermodynamics, and kinetics as well as on the changes in optical, dielectric, magnetic and electrical properties accompanying the transformations of a large number of inorganic solids. The subject of phase transformations in inorganic solids has been reviewed by Staveley [1],[1] Ubbelohde [2] and Rao [3, 4]. We shall now briefly describe the general features of crystal structure transformations.

Thermodynamics of Transformations. Classical thermodynamics gives a simple treatment of the equilibrium between two phases. The equilibrium properties of each phase are defined by the Gibbs free energy function, G, the pressure, P, and the temperature, T. The G–P–T surfaces of two phases are considered to be independent of each other and in a first order phase transformation the surfaces intersect at the transition point. If the transformation takes place from a low-temperature to a high temperature form, there will be an entropy increase and an associated change in volume during the transformation. The classical thermodynamic approach in describing phase transformations is inadequate since a variety of systems are known to exhibit transformations occurring over a wide range of temperatures. These systems show anomalous changes in specific heats and specific volumes and show evidence of "premonitory" phenomena. The transition temperature, T_t, in these transformations is taken to be that at which the heat capacity or the coefficient of expansion shows a maximum variation. This class of transformations which is not predicted by classical thermodynamics has often been referred to as "gradual, smeared or diffuse" transformations. Essentially, the difference between these transformations and the first order transformations described by classical thermodynamics lies in the nature or/and the magnitude of the discontinuity

*Supported by Project C–77 of the National Bureau of Standards under the Special International Programs.

[1] Figures in bracket indicate the literature references that appear at the end of each section.

of the thermodynamic energy functions and their derivatives.

In first order transformations, the difference in the free energies of the two phases is given by $0 = \Delta G = G_2 - G_1 = \Delta E - T\Delta S + P\Delta V$, where ΔE is the difference in internal energies of the two phases; if $P\Delta V$ in a transformation is small, one can compare the stabilities of the two phases in terms of their Helmholtz free energies: $0 = \Delta A = \Delta E - T\Delta S$. According to this equation, the transformation results from the compensation of the lattice energy difference by the entropy difference at T_t. At T_t, the free-energy curves intersect each other at $\Delta G = 0$. These phase transformations involve step-wise increase in energy with increase in temperature and show discontinuity in the energy as well as in many other properties of the system at T_t.

Many instances are known where phase transformations are induced by application of pressure; in these transformations the $P\Delta V$ term is very important. Wherever there is a decrease in volume during a transformation, pressure would favor such a transformation and the thermodynamic variables are simply correlated by the Clausius-Clapeyron equation. Since the phase produced by the application of pressure will have a lower volume, the decrease in volume is compensated by an increase in the ΔE or in the coordination number.

In the second- (or higher) order transformations, energy increases gradually with temperature until the rate of increase of energy sharply falls. As a result of this, discontinuity is found in specific heats or specific volumes. Since lambda-shaped specific heat curves are generally obtained in these transformations, these are also termed lambda-point transformations. Second- or higher-order transformations occur over a temperature interval and are generally associated with increase in disorder with rising temperature. If a solid has perfect order at absolute zero of temperature, a rise in temperature disturbs the order of the structure and with progressive increase in temperature, the structure gets more and more distorted until the transformation temperature T_t is reached. One can introduce an order parameter ξ which is equal to unity at absolute zero of temperature and becomes zero at T_t.

Although for the sake of definition one can classify transformations as first-order and second-order types, in reality it is difficult to find out exactly whether a transformation belongs to either of these two types. By definition first-order transformations should occur at one temperature and two phases of the same substance should not coexist at temperatures other than T_t. If a single crystal of a substance is taken through a transition point, the crystal should break up into a random assembly of one or more crystals of the other phase at T_t (depending on the magnitude of ΔV). If the temperature is then decreased below T_t, the first phase should reform randomly from the second phase (if the two phases are not crystallographically related). While transformations classified as first order are structurally discontinuous and involve drastic variations in energy, there are indications of higher order effects such as premonitory phenomena and thermal hysteresis in many of these transformations.

In continuous or second- (or higher) order transformations, premonitory changes are often found. Even though in these transitions there should be no discontinuity of structure, x-ray studies have shown that the two structures coexist over a narrow region of temperature. In some cases, transformations are found to proceed through the formation of "hybrid crystals" where the two structures coexist within a general pattern of orientation.

There are many phase transformations which strictly belong to neither first order nor to second order. For example, the ferroelectric transformation of KH_2PO_4 should theoretically be first order but conforms more closely to second order. The transformation of $BaTiO_3$ and related materials show lambda-like changes in properties as well as small changes in latent heat. There is superposition of second-order behavior on many first order transformations as in the transformation of alkali sulphates. It often happens that transformations have observable heat effects and yet the approach to the transformation is evidenced by a gradual change of properties. Even the order-disorder change in second order transformations may be seen as an abrupt change towards the termination.

Irreversible crystal structure transformations are found in many systems where one of the polymorphs is metastable in a particular temperature (or pressure) range. In such transformations, a polymorph transforms to the other form on heating above a particular temperature and remains in the new transformed structure even after cooling. It is not possible to assign any critical transformation temperature in an irreversible transformation and the transformation will be a function of time as well as temperature. One can only define a temperature below which a transformation does not take place. Typical examples of irreversible transformations are anatase-rutile (of TiO_2), aragonite-calcite (of $CaCO_3$) and cubic-hexagonal or cubic-monoclinic transitions of rare-earth sesquioxides. Many of these systems showing irreversible transformations are associated with small changes in internal energy, but large energies of activation may involve the breaking of the primary coordination or change in bond type.

Simple thermodynamic considerations indicate that one polymorph of a solid can be more stable under a specified set of conditions than the other. It should be realized, however, that it is difficult to strictly define the thermodynamic stability of a polymorph since a variety of physical factors as well as compositional differences affect the stability of polymorphs markedly. Thus, if there is any difference in the stoichiometry between two poly-

morphs, one cannot really classify them as belonging to the same polymorphic set. Similarly, if different samples of a solid contain different quantities of impurities, the regions of thermodynamic stability will vary.

A better insight into the nature of phase transformations can be obtained by correlating structural changes and the thermodynamics of transformations. The thermodynamics of transformations gives some indication as to the nature of structural changes accompanying transformations, but a better understanding can be obtained by considering the geometrical or crystallographic mechanisms. Since phase transformations in solids are associated with increase in entropy, one can visualize the structural origin of the entropy increases. For example, in first-order transformations, the phases with high internal energy and low density will have high entropy as well because of the greater magnitude of voids in the structure. In second-order or continuous transformations, the entropy changes have been related in many systems with the potential barrier to rotation. While going from the low- to the high-temperature forms in these systems, there will be some randomization of the structure. Ubbelohde [2] has discussed the structural origins of entropy increase in phase transformations in solids.

Structural Changes Accompanying Transformations. Buerger [5] has classified various types of thermal transformations based on structural changes involving the primary or higher coordination. Transformations where there are changes in the primary coordination will involve a more drastic change in energy and structure rather than those where there are changes only in the higher coordination. This can be visualized in the case of ionic crystals, where the energies of the ionic bonds vary inversely as the distance and the energies of the van der Waals bonds vary inversely as the sixth power of distance. Accordingly, one can classify transformations of the first order into two categories: first coordination transformations and higher coordination transformations.

Changes in primary coordination can take place by a reconstructive transformation, where the first coordination bonds are broken and reformed. Such transformations will involve high energies of activation and will be sluggish. Further, there may be no symmetry relation between the two phases. Reconstructive transformations give rise to large discontinuities such as cell dimensions, symmetry, internal energy, specific heat, etc. Changes in primary coordination may also take place through a dilatational mechanism as in the thermal transformation of cesium chloride (479 °C) or ammonium chloride (184 °C). Dilatational transformations are likely to be rapid compared to reconstructive transformations.

There are some transformations where only a part of the structure may undergo a change in the primary coordination. The ferroelectric transformations of barium titanate and lead titanate are likely to belong to this category since the coordination of titanium goes from 6 to 5 due to the shifting of the position of titanium from the center of the octahedron towards the vertex.

Many of the transformations involving changes in higher coordination may also have to proceed through the breaking of the primary bonds and for this reason, the energy changes and other features of the reconstructive transformations involving higher coordination may resemble those of the reconstructive first order transformations. In some transformations changes in higher coordination can be effected by a distortion of the primary bond. Such transformations may be called distortional or displacive transformations. These transformations will involve considerably smaller changes in energy and are usually fast. In the displacive transformations, the high temperature form is usually more open and has higher specific volume, specific heat and symmetry. In addition to the transformations discussed above, Buerger also discusses disorder transformations of two types: rotational and substitutional transformations.

Experimental Techniques Employed to Study Phase Transformations. A variety of techniques have been employed for the study of phase transformations in addition to x-ray diffraction which is an essential part of the study of any crystal structure transformation. Once a phase transition is identified in a solid by any technique, one has to investigate the same by other methods depending on the particular properties of interest. For example, the ferroelectric transformation of barium titanate has been investigated by the anomalies in heat capacity, breaks in thermal expansion curves and variations in optical properties (including vibrational spectra) in addition to changes in crystal structure and dielectric properties. The semiconductor-to-metal transitions in VO_2 and V_2O_3 have been studied by measurements of changes in magnetic susceptibility, heat capacity, electrical conductivity in addition to methods like nuclear magnetic resonance spectroscopy, Mössbauer spectroscopy, neutron diffraction, and differential thermal analysis. The transformation of KNO_2 provides another interesting example where a variety of methods of relevance have been employed to study the transformation. The reversible transition of KNO_2 was established by differential thermal analysis; x-ray diffraction was utilized to prove that the change was from monoclinic to cubic structure. Based on the crystal structures and also analogy with $NaNO_2$, it was suspected that the transformation was associated with a change from a ferroelectric to a paraelectric state. In fact, the dielectric hysteresis loop disappeared around 40 °C (Curie temperature, T_c); the dielectric anomaly was also observed at this temperature. A plot of electrical conductivity against temperature indicated a break at 40 °C. A study of the temperature-dependent infrared spectrum of KNO_2 showed

456-089 O - 72 - 2

that the absorbance of the NO_2 deformation frequency (830 cm^{-1}) showed a marked increase in intensity at the Curie temperature. This is similar to the behavior observed in the ferroelectric-paraelectric transformation of KNO_3. The literature has many such examples where several techniques have been employed to examine phase transformations in solids.

X-ray diffraction methods are by far the most important tools for the study of crystal structure transformations. Identification of structures of various phases by x-ray diffraction is very essential irrespective of what other techniques one employs to identify or examine the changes in the system accompanying the transformation. Single crystal work with Laue and Weissenberg photographs are particularly useful for a detailed knowledge of the mechanism of a phase transformation. Neutron diffraction has been employed effectively as a tool to examine the positions of light atoms as well as to study magnetic structures.

Both electronic and infrared spectroscopy are useful tools, provided a characteristic absorption band of the substance shows variations during a transformation. Wide-line NMR spectroscopy has been useful in the study of transformations containing suitable nuclei.

Measurements of (a.c. or d.c.) conductivity and dielectric constant are important techniques for the study of phase transformations. The transformations are generally indicated by a break in the conductivity *versus* temperature curves. Magnetic transitions (paramagnetic $\rightleftharpoons$ ferromagnetic or paramagnetic-antiferromagnetic) are generally studied by employing magnetic susceptibility measurements. Changes of magnetic anisotropy as a function of temperature has also been used to study polymorphic changes. Mössbauer spectroscopy containing (or doped with) the appropriate muclei provides valuable information on such transitions if the spectra are recorded at different temperatures.

Measurements of heat capacities as a function of temperature are valuable in the study of phase transformations (particularly in the case of second or higher order transitions). Differential thermal analysis is another powerful tool in the study of phase transformations. This technique has been employed to study the enthalpy change, activation energy and thermal hysteresis in transformations.

In principle, any technique that can measure a property of the substance which undergoes marked change during the transformation can be employed for the study of phase transformations. Dilatometric measurements, change in Young's modulus, thermal expansion of solids are some of the classical methods for the study of phase transformations.

References

[1] Staveley, L. A. K., Quart. Rev. (London) **3**, 64 (1949).
[2] Ubbelohde, A. R., Quart. Rev. (London) **11**, 246 (1957).
[3] Rao, C. N. R., and Rao, K. J., in Progress in Solid State Chemistry, Ed. H. Reiss, Vol. **4**, (Pergamon Press, Oxford, 1967).
[4] Rao, C. N. R., in Modern Aspects of Solid State Chemistry, Ed. C. N. R. Rao (Plenum Press, New York, 1970).
[5] Buerger, M. J., in Phase Transformations in Solids, Ed. R. Smoluchowski (John Wiley, New York, 1957) also see Fortschr. Mineral. **39**, 9 (1961).

1. Hydrogen Halides

Phase transitions of solid hydrogen halides have been investigated by many workers with a variety of experimental methods. The transitions generally take place at low temperatures. Dielectric relaxation, dielectric anomalies, specific heat, NMR and calorimetric measurements are some of the methods employed for these studies in addition to x-ray and neutron diffraction. While in HCl there is only one transition at ~ 98.36 K, in HBr and HI there are two transitions.

The transformation in HCl involves a change from the face centered cubic structure to a low symmetry structure (face centered orthorhombic); the transition is of first order. HBr undergoes two transitions, one at ~ 89 K (III → I) and the other at ~ 114 K (II → I). Phases III, II, and I are encountered successively when liquid HBr is cooled. The transition at 89 K is first order while the one at 114 K is a second order transition. Two transitions in HI are known at ~ 70.1 K (III → I) and at ~ 125.7 K (II → I); these are similar to the transitions in HBr. A third transition at 25 K has been reported in HI from infrared studies. The theory of phase transitions in hydrogen halides has been studied by Pauling and others. Some of these transitions are recently found to be associated with a change from a ferroelectric to a paraelectric state.

The gradual transitions in hydrogen halides were examined by Pauling [24] who attributed the transitions in HBr and HI to the incipient rotation about one crystal axis and the expansion of the crystal only along this axis. The difference between the low (α) and high (β) forms of HCl has been likened by Hettner [13], to that between liquids and solids. Molecules in the α-state vibrate about fixed and regularly oriented equilibrium positions while in the β-state only the equilibrium positions of several temporary groups are oriented with respect to one another. On the basis of classical mechanics, Kirkwood [17] accounts for the transitions in hydrogen halides, in terms of hindered rotation. The effects of dielectric relaxation during phase changes in hydrogen and deuterium halides have been discussed by Bauer [2]. Powels [28] has discussed the mechanism of transitions from a knowledge of the experimental results including those from calorimetric, dielectric, structural and thermal expansion measurements.

Krieger and James [19] proposed a model for a crystal exhibiting successive orientational or rota-

tional transitions as in hydrogen halides. The model consists of an array of classical rotors with next neighbor coupling. The nature of transitions in HCl, HBr, HI, DCl, DBr and DI have been successfully explained with this model. Recently, Kobayashi and co-workers [18] have suggested that the phase transitions in hydrogen halides can be understood qualitatively on the basis of a two dimensional rotational transition model with two sublattices.

The deuterium analogues of HCl, HBr and HI also exhibit transitions corresponding to those in hydrogen halides. Thus, DCl exhibits the II → I transition at ~ 105 K with an enthalpy of 320 cal · mol^{-1}; both DBr and DI exhibit the III → I transition at ~ 93.5 K (ΔH_{tr} ~ 169 cal · mol^{-1}) and ~ 77.3 K (ΔH_{tr} ~ 175 cal · mol^{-1}) respectively and the II → I transition at ~ 120 K (ΔH_{tr} ~ 303 cal · mol^{-1}) and ~ 128 K (ΔH_{tr} ~ 386.0 cal · mol^{-1}) respectively. The T_t and ΔH_{tr} are higher compared to those in the respective hydrogen analogues. Just as in hydrogen halides, phase transitions in the deuterium halides have been investigated by a variety of experimental methods.

Hydrogen Halides

Substances and measurement techniques	Data	Remarks	References
Hydrogen Chloride, HCl			
Calorimetric measurements like molar heat, specific heat etc., as a function of temperature	T_t ~ 98.36 K ΔH_{tr} ~ 284.3 cal · mol^{-1} ΔS ~ 2.89 e.u.	Transition is indicated by anomalies in molar heat or in the C_p *versus* T curves. The entropy of HCl was calculated to verify the third law.	[7,9].
X-ray and neutron diffraction	Cubic HCl has $a = 5.44 \pm 0.01$ Å at 98.5 K. At 85 K, solid HCl has a tetragonal form, with $c/a = 1.10$ where $a = 5.27$ Å, $c = 5.797$ Å. At 92.4 K, the structure is face centered orthorhombic with the space group, $Bb2_1m$. $a = 5.082$ Å, $b = 5.410$ Å, $c = 5.826$ Å. At 118.5 K, the structure is FCC, with $a = 5.482$ Å. (T_t ~ 98.4 K)	The $Bb2_1m$-space group indicates that HCl structure is non-centro symetric in this phase. The structure at 118.5 K is an average of disordered structures.	[22, 30].
NMR spectroscopy	Linewidth is measured as function of temperature.	The transition is found to be an order-disorder type. No evidence was found for a rotational transition.	[1].
IR spectra of crystalline HCl at 68 K, in KBr solvent	Two fundamental vibrations at 2704 and 2746 cm^{-1}, are observed. The angle H—Cl . . . H is ~ 107°.	The basic structural unit in HCl is a zigzag hydrogen bonded chain; the crystal appears to be built from anti-parallel pairs of such chains, but the relative position of the chains is uncertain.	[15].
Dielectric constant, ϵ, and tan δ measurements, as a function of temperature in various frequency ranges	T_t ~ 98.4 K	The dielectric behavior of solid HCl is predicted by Pauling's theory of free rotation of molecules in crystals. The dielectric behavior of liquid and disordered phases of HCl can be explained in terms of Onsager's equation.	[5, 35].
Dielectric hysteresis and ferroelectric behavior of solid HCl at low temperature	Spontaneous polarization, P_s, in HCl is 1.2 μc cm^{-2} at 90 K. The coercive field, E_c, is ~ 3.3 kV cm^{-1}. The ferroelectric loop disappears at ~ 98.4 K.	This observation seems to support Kobayashi's two sublattice theory of rotational transition in HCl.	[16].

Substances and measurement techniques	Data	Remarks	References
Hydrogen bromide, HBr			
Calorimetric measurements like molar heat, specific heat etc., as a function of temperature	T_t (III → I) ~ 90 K; (II → I) ~ 118 K; The ΔH_{tr} values are in the range 150–250 cal · mol^{-1}. Transitions are indicated by anomalies in C_p versus T curves.	The ΔH_{tr} values are not consistent with other experimental results. The transitions are probably akin to those in NH_4Cl.	[7, 10]
X-ray diffraction	Existence of solid HBr in the (space group V^7 or V_h^{23} i.e., D_2^7 or D_{2h}^{23} structure in the 85–90 K range is established beyond doubt. Below ~ 100 K a=5.76 Å. Below 100 K, HBr exhibits rhombic symmetry with axial ratios, a:b:c=0.985:1:1.075, where a=5.555 Å, b=5.64 Å and c=6.063 Å; Z=4; ρ=2.81 g cm^{-3}.	The x-ray studies of Ruhemann and Simon [29] between 82–120 K, however, do not indicate any fundamental crystallographic changes during the transition. They propose a FCC structure throughout this temperature range.	[22, 23, 29].
NMR spectroscopy	Line width is measured as a function of temperature.	A basic factor affecting the line width is the characteristic flipping time i.e., the average time to change its orientation. The results suggest that the phase transition in HBr is an order-disorder type.	[1].
Infrared of HBr crystals at 68 K.	Two fundamental vibrations at 2404 and 2438 cm^{-1} are observed.	The basic structural unit in HBr crystals is a zigzag hydrogen bonded chain.	[15].
Measurement of ϵ as a function of frequency, ω and temperature	ϵ varies with ω only below 95 K. The dispersion domains are displaced towards the high frequency with T. One of the dispersions is of constant amplitude while the other is temperature dependent, and exists even after T_t. Definite hysteresis effects were observed in the transitions.	In addition to the two dispersions mentioned, a third one was indicated at higher frequencies. A rotation tunnel effect is introduced to explain the variation of the critical frequency with temperature. Such an effect is shown to be present in HBr.	[6, 25, 26, 27].
ϵ and tan δ measurements	The sharp increase in ϵ suggests a first order transition at ~89.8 K while a sharp increase in tan δ suggests a second order transition at ~113.6 K.	The complex ϵ is ascribed to a skewed arc function found for the low-temperature phase. Deviations of the relaxation rates can be explained in terms of cooperative interaction effects in the disordered phase.	[12, 20]
Static dielectric constant and dispersion loss measurements.	ϵ_{stat} above 117 K agrees well with Onsager's equation. In phase II, ϵ rises to peak value of 200 at 89 K and falls to 32 at ~72 K in phase III.	Phase transitions are indicated by anomalies in ϵ.	[3].
Dielectric hysteresis in HBr single crystals.	The polarization versus field curves show a ferroelectric hysteresis loop. The measured spontaneous polarization, P_s, is about 0.4 μc cm^{-2} and the coercive field, E_c is ~4.3 KV cm^{-1}.	The phase transition in HBr i.e., the second order change is thus possibly associated with a change from ferroelectric to paraelectric state thus conforming to the two sublattice model of Kobayashi.	[16].
Effect of ultrasonic waves on thermal hysteresis of transition in HBr.	The hysteresis is not affected by ultrasonic waves or by inoculation.	The position of the equilibrium curve in the transition interval could not be determined.	[8].

Substances and measurement techniques	Data	Remarks	References
Hydrogen iodide, HI			
Calorimetric measurements like molar heat, specific heat etc., as a function of temperature	For III → I, T_t, 72 K; $\Delta H_{tr} \sim 150$ cal · $^{-1}$, II → I, T_t, ~ 124 K; $\Delta H_{tr} \sim 395$ cal · mol^{-1}.	The transitions are indicated by anomalies in the molar heat/C_p versus temperature curves.	[7, 11].
X-ray diffraction	HI has a face centered tetragonal structure with $c/a = 1.08$ ($a = 6.10$ Å) at ~ 100 K. This structure changes to a FCC structure above 127 K: $a = 6.19$ Å at 125 K; $\rho = 3.17$ g cm^{-3}.	The transitions in HI may be similar to those in NH_4Cl.	[21, 22, 23, 29].
NMR Spectroscopy	The line width is measured as a function of temperature.	The line width is affected by the average time the molecules take to change from one orientation to another. This indicates the nature of the transition to be an order-disorder type.	[1].
Infrared study of a new phase transition in HI, in the range 6 to 79 K.	At 25 K, HI undergoes a phase change to a phase with more molecules in the unit cell and also the phase below 25 K is one of less symmetry than the high phase above 25 K.	The transition at 25 K is readily reversible and rapid. No hysteresis is evidenced in these studies.	[14].
Deuterium chloride, DCl			
Calorimetric measurement of molar heat of DCl.	$T_t \sim 105.03$ K, $\Delta H_{tr} \sim 320.1$ cal · mol^{-1}	Both T_t and ΔH_{tr} are higher than in HCl. The transition is probably a first order one.	[4].
X-ray and neutron diffraction (as well as heat capacity measurement).	$T_t \sim 105$ K. At 92.4 K, the structure is face-centered orthorhombic, with $a = 5.0685$ Å, $b = 5.3990$ Å and $c = 5.828$ Å. At 118.5 K. The structure is face-centered cubic with $a = 5.475$ Å. The space group at 77 K is Bb2$_1$m (same as HCl).	The FCC structure at 118.5 K is only an average of disordered structures, similar to that in HCl. On the other hand the unit cell of DCl shows an anisotropic reduction in lattice constants compared to HCl.	[30].
Deuterium bromide, DBr			
Calorimetric measurement of molar heat as a function of temperature.	$T_t \sim 93.5$ K (III → I) $\Delta H_{tr} \sim 196.7$ cal · mol^{-1}. $T_t \sim 120.26$ K. $\Delta H_{tr} \sim 303$ cal · mol^{-1}. $T_t \sim 128.28$ K, $\Delta H_{tr} \sim 386.4$ cal · mol^{-1}.	The T_t and ΔH_{tr} are higher than in HBr. The second transition appears to go through a metastable state.	[4].
X-ray and neutron diffraction (as well as heat capacity).	Two second order transitions at ~ 93.5 K (III → I) and at ~ 120.3 K (II → I) are noticed. At 84 K, the space group is Bb2$_1$m while at 107 K the space group is Bbcm. At 84 K, the structure is orthorhombic with $a = 5.44 \pm 0.02$ A, $b = 5.614 \pm 0.005$ Å, and $c = 6.12 \pm 0.005$ Å; $z = 4$. At 107 K, the structure is orthorhombic with $a = 5.559 \pm 0.005$ Å, $b = 5.649 \pm 0.005$ Å, and $c = 6.095 \pm 0.005$ Å.	Below 93.5 K, DBr is isomorphous with DCl (i.e., it has an ordered crystal structure, composed of parallel zig-zag chains). Between 93.5 K and 120.3 K, DBr has a disordered structure where the disorder is orientational with two equilibrium orientations for each molecule.	[31]
Kinetics of DBr transition at 93.5 K by x-ray and neutron diffraction methods.	$T_t \sim 93.5$ K $\Delta V \sim 3.66$ Å^3 per unit cell. $\Delta V/V_0 \sim 1.94$ percent. A hysteresis of about 0.60 was observed.	Kinetics and the nature of the transition are discussed in terms of these experimental results.	[32]

Substances and measurement techniques	Data	Remarks	References
Deuterium iodide, DI			
Calorimetric measurement of molar heat as a function of temperature.	$T_t \sim 77.3$ K (III → I); $\Delta H_{tr} \sim 175.6$ cal·mol^{-1}. $T_t \sim 128.28$ K (II → I); $\Delta H_{tr} \sim 386.4$ cal·mol^{-1}.	T_t and ΔH_{tr} are higher than for HI transitions.	[4, 34].

References

[1] Alpert, N. L., Phys. Rev. **75**, 398 (1949).
[2] Bauer, E., compt. rend. 272 (1952).
[3] Brown, N. L., and Cole, R. H., J. Chem. Phys. **21**, 1920 (1953).
[4] Clusius, K., and Wolf, G., Z. Naturforsh **2a**, 495 (1947).
[5] Cone, R. M., Denison, G. H., and Kemp, J. D., J. Am. Chem. Soc. **53**, 1278 (1931).
[6] Damköhler, G., Ann. Physik. **31**, 76 (1938).
[7] Eucken, A., and Karwat, E., Z. physik. Chem. **112**, 467 (1924).
[8] Eucken, A., and Güttner, W., Math. physik., Klasse, Fachgruppe. II [N.F.] **2**, 167 (1937).
[9] Giauque, W. F., and Wiebe, R., J. Am. Chem. Soc. **50**, 101 (1928).
[10] Giauque, W. F., and Wiebe, R., J. Am. Chem. Soc. **50**, 2193 (1928).
[11] Giauque, W. F., and Wiebe, R., J. Am. Chem. Soc. **51**, 1441 (1929).
[12] Groenewegen, P. P. M., and Cole, R. H., J. Chem. Phys. **46** (3), 1069 (1967).
[13] Hettner, G., Ann. physik **32**, 141 (1938).
[14] Hiebert, G. L., and Hornig, D. F., J. Chem. Phys. **26**, 1762 (1957).
[15] Hornig, D. F., and Osberg, W. E., J. Chem. Phys. **23**, 662 (1955).
[16] Hoshino, S., Shimaoka, K., and Nümura, N., Phys. Rev. Letters **27**, 1286 (1967).
[17] Kirkwood, J. G., J. Chem. Phys. **8**, 205 (1940).
[18] Kobayashi, K. K., Hanamura, E., and Shishido, F., Phys. Letters **28A**, 718 (1968).
[19] Krieger, T. J., and James, H. M., J. Chem. Phys. **22**, 796 (1954).
[20] Lacerda, L., and Brot, C., compt. rend. **236**, 916 (1953).
[21] Mauer, F. A., Keffer, C. J., Reeves, R. B., and Robinson, D. W., J. Chem. Phys. **42** (2), 1465 (1965).
[22] Natta, G., Nature **127**, 235 (1931).
[23] Natta, G., Gazz. Chim. ital, **63**, 425 (1933).
[24] Pauling, L., Phys. Rev. **36**, 430 (1930).
[25] Powles, J. G., compt. rend. **230**, 836 (1950).
[26] Powles, J. G., Nature **165**, 686 (1950).
[27] Powles, J. G., J. Phys. Radium **13**, 121 (1952).
[28] Powles, J. G., Trans. Faraday Soc. **48**, 430 (1952).
[29] Ruhemann, B., and Simon, F., Z. physik. **B15**, 389 (1932).
[30] Sandor, E., and Farrow, R. F. C., Nature **213**, 171 (1967).
[31] Sandór, E., and Johnson, M. W., Nature **217**, 541 (1968).
[32] Sandór, E., and Johnson, M. W., Nature **223**, 730 (1969).
[33] Smyth, C. P., and Hitchcock, C. S., J. Am. Chem. Soc. **55**, 1830 (1933).
[34] Staveley, L. A. K., Quartr. Rev. **3**, 64 (1949).
[35] Swenson, R. W., and Cole, R. H., J. Chem. Phys. **22**, 284 (1954).

2. Alkali Halides

All the alkali halides with the exception of CsCl, CsBr, and CsI crystallize in the NaCl structure (Fm3m), the three cesium halides crystallizing in the CsCl structure (Pm3m). CsCl undergoes a first order phase transformation at ~480 °C (at 1 atm pressure) from the Pm3m structure to the Fm3m structure. The transformation in CsCl is reversible and is associated with considerable thermal hysteresis, ΔT, as well as an appreciable change in molar volume, ΔV. The transformation of CsCl is likely to proceed by a mechanism involving dilatation along the body diagonal; the role of lattice vacancies in the mechanism of transformation is not clearly established. The phase transition in CsCl has been studied with the aid of a variety of experimental tools. Fm3m structures for CsBr, and CsI have been reported in evaporated thin films at low temperatures. No other transformation data are available for CsBr, CsI, or CsF.

No phase transformations are known in lithium halides. Pressure transformation (from Fm3m to Pm3m) data have been reported for sodium, potassium and rubidium halides. The thermal transformation data on CsCl as well as the pressure transition data on other alkali halides have been employed to evaluate the lattice energies of the halides in the Pm3m and Fm3m phases. The Born treatment of ionic solids have been employed with fair success to explain the relative stabilities of the Pm3m and Fm3m phases.

The phase transformation in CsCl at 753 K involves a change from the Pm3m structure to the NaCl structure. Menary, Ubbelohde and Woodward [40] suggested that a large increase in vacancies occured in the neighborhood of the transition temperature. However, Hoodless and Morrison [21] showed from electrical conductivity measurements that the transitions may not involve a disruption of the lattice and that the mechanism is likely to be dilatational as suggested by Buerger [10].

The Born-Mayer model [23] has been widely employed to calculate the lattice energies of ionic solids especially of alkali halides. May [38] employed a three-parameter repulsive term and a higher van der Waals contribution to account for the greater stability of the Pm3m phase of CsCl. The use of a higher van der Waals term was criticized by Tosi and Fumi [68, 69] who employed structure-dependent repulsive parameters to account for the phase transition in CsCl. Recently, Rao and co-workers [45, 60–62] have employed a four parameter repulsive term in the Born treatment to explain the phase transition in CsCl. The model also accounts for the stabilization of the Fm3m phase by added KCl or RbCl as well as for the opposite behavior of the CsCl + CsBr solid solutions [45, 60].

It is definitely established that all the potassium and rubidium halides with the likely exception of the fluorides undergo pressure transformations from the NaCl structure (Fm3m) to the CsCl structure (Pm3m) [7, 25, 47]. The product of the volume change, ΔV, accompanying the transition and the transition pressure, P, may be taken to be equal to the difference between the lattice energies of the two structures at the transition pressure [25]. Several workers have attempted to calculate the lattice energy differences between the two phases with the aid of the Born model of ionic solids. Structure-dependent [68, 69] as well as the four-parameter [62] repulsive terms in the Born-treatment have been employed to explain these transformations. The need for a higher van der Waals term in the Born model to account for the transition energies of KX and RbX (X = Cl, Br or I) has been pointed out [62]. An atomistic formulation of compressibility has also been used to discuss the pressure transitions of alkali halides [53]. Madan and Sharma [65] have calculated the lattice energies of all the alkali halides with the Lennard-Jones (12:6) potential.

Alkali Halides

Substances and measurement techniques	Data	Remarks	References
Sodium fluoride, NaF (Fm3m, a = 4.6344 Å at 299 K)			
Volumetric investigation of high pressure transformation in NaF.	Transition begins at ~18.3±1 kbar and 430.5 K. $\Delta V \sim 5\%$.	Transition is reversible and incomplete even at 45 kbar.	[48].
Quantum mechanical calculation. (with nearest neighbor repulsion only) of transition pressures for NaF and NaCl for the Fm3m-Pm3m change.	$P_T \sim 280$ kbar.	The value is slightly different from the known experimental data.	[37].
Sodium chloride, NaCl (Fm3m, a=5.6402 Å at 299 K)			
X-ray investigation of the high pressure transformation employing a diamond anvil (up to ~18 kbar)	P_T, 17.5–18 kbar a (Fm3m)=3.36±0.04 Å at 298 K and 1 atm. $\Delta V \sim -1.0 \pm 0.05$ cm^3 mol^{-1} $\Delta S \sim 1.5 \pm 0.3$ cal·deg^{-1}·mol^{-1}.	An extreme value of 300 kbar is also reported for P_T. Experimental and calculated transition pressures are compared for some more halides.	[4, 17, 18, 28].
Latent heat of the Fm3m–Pm3m transformation from the temperature dependence of P_T up to 473 K.	$\Delta H_{tr} \sim 660 \pm 370$ cal·mol^{-1} at 298 K.	The ΔH_{tr} is comparable to the ΔH_{tr} for the thermal transition of CsCl.	[50].
Dilatometric study on NaCl single crystals with organosilicon liquids as the dilatometric medium.	$P_T \sim 21$ kbar at 613 K ~25 kbar at 803 K $(\partial P/\partial T)$ is positive.		[12].
Shear induced transition in shock loaded NaCl employing a piezo-electric quartz (up to 30 kbar).	Fm3m–Pm3m transition occurred and conformed to a first order.	NaCl is unreliable as a high-pressure gauge.	[1, 33].
Equation of state for NaCl between 0–500 kbar and 273–1773 K.	Pressure as a function of lattice constant and temperature are obtained for the equation of state.		[15, 16].
Dielectric constant and elastic constant measured as a function of pressure up to ~25 kbar at room temperature.	No anomaly (characteristic of a structural change) was found in elastic or dielectric constants.		[11].

Substances and measurement techniques	Data	Remarks	References
Sodium bromide, NaBr (Fm3m, a=5.9772 Å at 299 K)			
High pressure transition by volume discontinuity method.	$P_T \sim$ 10–14 kbar at 473 K.	The transition is very sluggish.	[49, 52].
Sodium iodide, NaI (Fm3m, a=6.4728 Å at 299 K)			
Temperature dependence of transition pressure.	$P_T \sim$ 10–14 kbar, at 473 K. There is a transition to the Pm3m structure.		[52].
Volume discontinuity method upto ~ 50 kbar and 437 K.	$P_T \sim 10.00 \pm 2.5$ kbar at 437 K; $\Delta V \sim 8\%$.		[49].
Potassium fluoride, KF (Fm3m, a = 5.347 Å at 299 K)			
High pressure transition investigated by x-rays.	$P_T \sim$ 88 kbar from theory	No experimental P_T is known for KF.	[17].
Lattice energies are evaluated for both Pm3m and Fm3m structures. P_T is estimated from available pressure transition data (calcd).	$P_T \sim$ 20 kbar		[73].
Potassium chloride, KCl (Fm3m, a = 6.2931 Å at 298 K)			
High pressure studies on KCl and x-ray investigation.	$P_T \sim$ 19–20 kbar. $\Delta V \sim 0.055$ cm^3 g^{-1} $\Delta H_{tr} \sim -10.0 \pm 8$ cal · mol^{-1}. a(Pm3m) = 3.61 Å at 32 kbar.	Lattice energies are estimated for both Pm3m and Fm3m structures to explain the stability etc.	[7, 27, 30, 50, 44, 73].
Optical method—by noting the shift in the vibrational frequency of an added ion like CN^- in KCl crystal subjected to pressure.	$P_T \sim$ 19–30 kbar	Transition is indicated by a decrease in the transparency of the salt at P_T.	[31, 66].
Calculation of P_T from experimental data on coefficient of thermal expansion and compressibility.	$P_T \sim$ 22–36 kbar. $\Delta V/V \sim 0.08$		[17, 64].
Potassium bromide, KBr (Fm3m, a = 6.60 Å at 298 K)			
Pressure transition in KBr by volume discontinuity method.	$P_T \sim$ 17–19.3 kbar. $\Delta V \sim 0.0325$ cm^3 g^{-1}.	Transition pressure is independent of temperature. Transition is sluggish at room temperature. Around 323 K, hysteresis is about 30 bar. The experimental data are in agreement with Bridgman's reports [7].	[7, 30, 52].
Optical study of polymorphic change under pressure.	$P_T \sim$ 18 kbar. Transition was observed by noticing an abrupt change in the transmission of the material as it passes through the phase transition. Also, the transition was indicated by a discontinuity in the shift of the vibrational frequency of the added CN^- ion.		[31, 66].
Calculation of P_T.	$P_T \sim$ 18 kbar		[73].

Substances and measurement techniques	Data	Remarks	References
Potassium iodide, KI (Fm3m, $a=7.0655$ Å at 298 K)			
High pressure studies on KI. Diamond squeezers are usually employed in addition to piston displacement and volume discontinuity method etc., and examined by x-ray.	P_T 18–21 kbar. Transition is almost complete around 24 kbar. Internal pressure in KI after the transition is ~ 20.8 kbar as estimated from $\Delta V/V_0$ value. $a_{Pm3m}=4.13\pm0.02$ Å at 298 K.	The value of P_T agrees well with calculated value of 21 kbar. P_T appears to be independent of temperature. Transition is sluggish at 298 K but faster at 423 K.	[7, 26, 17, 30, 52. 73].
Rubidium fluoride, RbF (Fm3m, $a=5.64$ Å at 298 K; a lower value of a has been reported by Lew [33a]).			
Pressure temperature curves for RbF.	$P_T\sim22$ kbar at ~973 K.	Transition takes place to the Pm3m structure.	[51].
Estimation of P_T	$P_T\sim11.76$ kbar.		[73].
Rubidium chloride, RbCl (Fm3m, $a=6.5810$ Å at 300 K).			
Thin layers of RbCl evaporated onto amorphous bases at low temperatures and examined by electron diffraction.	$a_{Pm3m}=3.97$ Å at 193 K.	The Pm3m phase slowly disappears as the temperature is increased.	[5].
High pressure transition in RbCl and x-ray investigation.	$P_T\sim31$ kbar (calculated) ~ 5 kbar at 133 K (observed) ΔH_{tr} 130±20 cal·mol^{-1}. P_T is ~ 7.5 kbar at 973 K.	The volume contraction in RbCl is comparable to that in CsCl for the Pm3m–Fm3m phase. Thus the high pressure phase of RbCl is CsCl type only.	[6, 17, 24, 47, 50, 51, 68, 69].
Investigation of pressure effects on the compressive strength and stress-strain behavior of RbCl.	$P_T\sim7.5$ kbar. A simultaneous deformation and polymorphic transformation were observed.	The simultaneous deformation and transformation are attributed to the crack-healing effect. Cracks appear at about 1% deformation and vanish in large deformations. especially at the buckled surface of the sample. At pressures above P_T, the cracks do not disappear but transform to a system of slanted fissures.	[34].
Rubidium bromide, RbBr (Fm3m, $a=6.889$ Å at 298 K)			
Thin layers of RbBr evaporated onto amorphous bases and examined by electron diffraction at low temperatures.	$a_{Pm3m}=4.24$ Å at 230 K.	The intensity of the Pm3m lines disappear with rise in temperature.	[5].
Pressure transition in RbBr by x-ray investigation, in the range 0–40 kbar and 273–873 K.	$P_T\sim25$ kbar (theory) ~ 4.6 kbar (observed). ~ 5.5 kbar at 873 K.	The experimental observations can be fitted to Simon equation.	[6. 17, 47, 51, 52].
RbBr grown from aqueous solution on oriented silver films and x-ray investigation.	The films have RbBr with Pm3m structure where $a=4.06$ Å. If the film is grown from vapor, the structure is Fm3m.	Vapor grown RbBr films change to Pm3m if dissolved in water and grown from solution on silver films.	[64].

456-089 O - 72 - 3

Substances and measurement techniques	Data	Remarks	References
Rubidium iodide, RbI (Fm3m, $a = 7.342$ Å at 300 K)			
Thin layers of RbI evaporated onto amorphous bases and examined by electron diffraction.	$a_{Pm3m} = 4.59$ Å at 193 K.	The intensity of the Pm3m lines slowly disappears as the temperature is increased.	[5].
Pressure-temperature curves for RbI from 0–40 kbar and 273 to 873 K.	$P_T \sim 4.8$ kbar at 873 K, above which the Pm3m phase is possible	The experimental points fit to Simon equation.	[51].
Optical investigation of the Fm3m-Pm3m pressure transition in RbI single crystals. A high pressure vessel with a modified Vickers metallographic microscope and time lapse photographic technique are employed.	$P_T \sim 3.5$ kbar.	The transition was affected by the nature of the crystal surfaces. The lattice dynamics of the transition has been discussed in terms of the shifts in the optical and acoustical mode frequencies. Results of this discussion are not compatible with the experimental thermal expansion data on RbI.	[13, 14].
Dilatometric studies of the Fm3m-Pm3m transition in RbI; construction of the P–T diagram.	$P_T \sim 4.3$ kbar at 298 K. $(dT/dP) = 1.4°$ bar^{-1} for the equilibrium curve.	Hysteresis effects are observed in the transition.	[54].
Cesium chloride, CsCl (Pm3m, $a = 4.123$ Å at 298 K)			
Calorimetric methods	T_t, 743 K ΔH_{tr}, 580–707 cal · mol^{-1}		[2, 29, 32].
Application of the Clausius-Clapeyron relation to the transition.	The relation is applicable with limited utility.		[36].
DTA of pure CsCl and solid solutions with other alkali halides and x-ray diffraction studies of CsCl transition at various temperatures.	Transition (T_t, 745–753 K) is of first order ΔH_{tr}, 600–880 cal · mol^{-1}; $\Delta T \sim 33°$; $\Delta V \sim 7.34$ cm^3 mol^{-1}. With incorporation of KCl or RbCl, the T_t and ΔH_{tr} are decreased with increase in KCl or RbCl. With CsBr, T_t and ΔH_{tr} are increased.	The Fm3m phase of CsCl gets stabilized at ordinary temperatures in solid solutions with 30% KCl or 35% RbCl. With KCl or RbCl solid solutions, first order characteristics of the CsCl transition are still preserved. In CsBr solid solutions higher order components are present in the transition and the Pm3m structure is retained at ordinary temperatures.	[45, 56, 59, 60, 73].
Temperature variable x-ray diffraction studies on CsCl powder as well as single crystals.	T_t, 742–753 K. The lattice const. extrapolated to 298 K is, $a = 6.91$ Å for the Fm3m phase (at 753 K, $a = 7.02$ Å). In CsCl + CsBr solid solutions coexistence of Pm3m and Fm3m phases is observed in the x-ray patterns in the neighborhood of the transition temperature.	The lattice constants of the Pm3m as well as the Fm3m phases decrease with increasing percent of KCl or RbCl. On the other hand the lattice constant increases with CsBr content. The molar volume change, ΔV, slightly increases in KCl solid solutions indicating that the transitions are first order. In CsBr solid solutions, ΔV decreases indicating the presence of higher order components in these transitions.	[22, 23, 40, 45, 57, 58, 71, 74, 75].
Electron diffraction studies of CsCl transition.	T_t, 753 K; $a_{Fm3m} = 6.923$ Å at 227 K and 6.940 Å at 298 K (extrapolated values).	The transformation is believed to proceed through a defect mechanism. Hybridization and mixed crystal (of both Pm3m and Fm3m structures) formation were noticed just below T_t.	[5, 41, 63].

Substances and measurement techniques	Data	Remarks	References
Ionic conductivity measurements of CsCl and its solid solutions with KCl, RbCl, CsBr and $SrCl_2$.	The T_t is indicated by a break in the log σ versus $1/T$ plots. The activation energies from the plot give values of cation migration energy, $E_c^m \sim 0.6$ eV and Schottky defect formation energies, E_s. $E_s \sim 1.4-1.8$ eV in pure CsCl in Pm3m phase. The value of E_s in the Fm3m phase. is ~ 2.0 eV. The cation migration energy decreases slightly with K^+ or Cs^+ content and increases with Br^- content. Addition of Sr^{+2} slightly decreases the T_t of CsCl.	The conductivity experiments on single crystals as well as polycrystalline pellets give results which do not vary much. The role of vancancies in the mechanism of the transition is not definitive. Though vancancies may aid the transition by decreasing the T_t, the mechanism would still involve dilatation along the body diagonal.	[3, 42, 43, 46, 46a, 72].
Self-diffusion and electrical conductivity measurements.	E_a for conduction ~ 1.26 eV; E_a for diffusion: 1.53 eV for Cs^{127} 1.27 eV for Cl^{36}.	Conduction is only ionic. Schottky defects are predominant. The transformation does not involve an extensive disruption of lattice. The transformation is essentially dilatational with an increase in lattice vacancies around T_t.	20, 21].
Electronographic investigation of evaporated thin films.	Both Pm3m and Fm3m structures were noticed.		[19].
Study of the phase transition by S^{35} emanation from $CsCl^{35}$ and its solid solution with CsBr.	T_t is indicated by the increased radioactivity. T_t is increased by CsBr addition.		[35].
Kinetics of the CsCl transition above 733 K, by electron diffraction studies.	The kinetics become difficult to follow because CsCl starts to sublime at ~ 730 K and is extremely sensitive to moisture.	Both Pm3m and Fm3m phases coexist near T_t.	[70].
Cesium bromide, CsBr, (Pm3m, $a=4.2953$ Å at 298 K)			
X-ray diffraction up to melting point.	Some extra weak lines are observed in the x-ray spectra, which do not belong to the Pm3m structure.	The weak lines are with 2 to 4 times the basic lattice period of the stable Pm3m structure.	[55, 71].
Thin films of CsBr evaporated on to surface of mica, $CaCo_3$ or amorphous bases at low temperatures and examined by electron diffraction.	Fm3m structure of CsBr was noticed $a=7.2300$ Å -7.253 Å at ~ 155 K.	The Fm3m lines are of weak intensity and disappear with time.	[5, 63].
Evaluation of T_t and ΔH_{tr} from experimental data from CsCl+CsBr solid solutions and thermodynamic considerations.	For CsBr, $T_t \sim 1153$ K for Pm3m–Fm3m transition; ΔH_{tr} (calcd)=300 cal · mol^{-1}.	The transition temperature is higher than the melting point of CsBr.	[72].
Cesium iodide, CsI (Pm3m, $a=4.5679$ Å at 299 K)			
X-ray diffraction of CsI up to the melting point.	No transition was observed.		[71].
Thin films of CsI evaporated on to amorphous bases or mica or $CaCO_3$ at very low temperatures and examined by electron diffraction.	Both Pm3m and Fm3m structures were observed with the intensity of Fm3m structures becoming weak with time. $a_{Fm3m}=7.631$ Å at 148 K.	The intensity of the lines due to the Fm3m structure weakens slowly with increase of temperature and completely disappears at room temperature.	[5, 63].

Substances and measurement techniques	Data	Remarks	References
CsI evaporated on to K and Rb halides (as thin films) and examined by electronograph.	Microcrystals of NaCl and CsCl type structures were observed. With increasing thickness of the CsI films the lines due to Pm3m structure increase in intensity.	Microcrystals of Fm3m structure were unstable in air and recrystallized into Pm3m structure. Exchange of Cs and Rb cations was observed to take place in the presence of moisture.	[19].

References

[1] Al'tshuler, L. V., Brazhnik, M. I., German, V. N., and Mirkin, L. I., Sov. Phys. Solid State **9**, 2417 (1968).
[2] Arell, A., Roiha, M., and Aaltonen, M., Phys. Kondens. Materie. **6**, 140 (1967).
[3] Arends, J., and Nijboer, H., physica stat. sol. **26**, 537 (1968).
[4] Bassett, W. A., Takahashi, T., Mao, H., and Weaver, J. S., J. Appl. Phys. **39**, 319 (1968).
[5] Blackman, M., and Khan, I. H., Proc. Phys. Soc. (London) **77**, 471 (1961).
[6] Bridgman, P. W., Z. Krist. **67**, 363 (1928).
[7] Bridgman, P. W., Phys. Rev. **48**, 893 (1935).
[8] Bridgman, P. W., Proc. Am. Acad. Arts Sci. **76**, 1 (1945)
[9] Buckle, E. R., Diss. Faraday Soc. **30**, 46 (1960).
[10] Buerger, M. J., in Phase Transformations in Solids, Ed. R. Smoluchowski (John Wiley & Sons. Inc., New York, 1951).
[11] Corll, J. A., and Samara, G. A., Solid State Communications **4**, 283 (1966).
[12] Davis, L. A., and Gordon, R. B., phys. stat. sol. **36**, K133 (1969).
[13] Daniels, W. B., and Skoultchi, A. I., J. Phys. Chem. Solids. **27**, 1247 (1966).
[14] Daniels, W. B., J. Phys. Chem. Solids. **28**, 350 (1967).
[15] Decker, D. L., J. Appl. Phys. **36**, 157 (1965).
[16] Decker, D. L., J. Appl. Phys. **37**, 5012 (1966).
[17] Evdokimora, V. V., and Vereschagin, L. F., Sov. Phys. JETP **16**, 855 (1963).
[18] Evdokimora, V. V., and Vereschagin, L. F., Zh. Eksperim. i. Teor. Fiz. **43**, 1208 (1962).
[19] Haav, A., Trudy. Inst. Fiz. i Astron. Akad. Nauk. Eston. S.S.R., page 123 (1961).
[20] Harvey, P. J., and Hoodless, I. M., Phil Mag. **16**, 543 (1967).
[21] Hoodless, I. M., and Morrison, J. A., J. Phys. Chem. **66**, 557 (1962).
[22] Hovi, V., Ann. Univ. Turkuensis, Ser. A I **26**, 8 (1957); Acta. Met. **6**, 254 (1958).
[23] Huggins, M. L., and Mayer, J. E., J. Chem. Phys. **1**, 637 (1933).
[24] Jacobs, R. B., Phys. Rev. **54**, 325 (1938).
[25] Jacobs, R. B., Phys. Rev. **54**, 468 (1938).
[26] Jamieson, J. C., J. Geol. **65**, 334 (1957).
[27] Jamieson, J. C., and Lawson, A. W., J. Appl. Phys. **33**, 776 (1962).
[28] Johnson, Q., Science **153**, 419 (1966).
[29] Kaylor, C. E., Walden, G. E., and Smith, D. F., J. Phys. Chem. **64**, 276 (1960).
[30] Kennedy, G. C., and La Mori, P. N., J. Geophys. Res. **67**, 851 (1962).
[31] Klynev, Yu. A., Dokl. Acad. Nauk. S.S.S.R. **144**, 538 (1962).
[32] Krogh-Moe, J., J. Am. Chem. Soc. **82**, 2399 (1960).
[33] Larson, D. B., Keeler, R. N., Kusubov, A., and Hord, B. L., J. Phys. Chem. Solids **27**, 476 (1966).
[33a] Lew, H., Can. J. Phys. **42**, 1004 (1964).
[34] Livshits, L. D., Beresnev, B. I., Genshaft, Yu. S., and Ryabinin, Yu. N., Dokl. Acad. Nauk. S.S.S.R. **164**, 541 (1965).
[35] Makarov, L. L., Aloi, A. S., and Stupin, D. Yu., Radiokhimiva **11**, 116 (1969).
[36] Majumdar, A. J., and Roy, R., J. Inorg. Nucl. Chem. **27**, 1961 (1965).
[37] Mansikka, K., Ann. Univ. Turku. Ser. A I **121**, 11 (1968).
[38] May, A., phys. Rev. **52**, 339 (1937); *ibid.* **54**, 629 (1938).
[39] Mayer, J. E., J. Chem. Phys. **1**, 270 (1933).
[40] Menary, J. W., Ubbelohde, A. R., and Woodward, I., Proc. Roy. Soc. (London) **A208**, 158 (1951).
[41] Morlin, Z., and Tremmel, J., Acta. Phys. **21**, 129 (1966).
[42] Morlin, Z., Acta. Phys. **21**, 137 (1966).
[43] Morlin, Z., Acta. Phys. **24**, 277 (1968).
[44] Nagasaki, H., and Minomura, S., J. Phys. Soc. Japan **19**, 1496 (1964).
[45] Natarajan, M., Rao, K. J., and Rao, C. N. R., Trans. Faraday Soc. **66**, 2497 (1970).
[46] Natarajan, M., Ph.D., Thesis, 1970, Indian Institute of Technology, Kanpur, India.
[46a] Natarajan, M., Prakash, B., and Rao, C. N. R., J. Chem. Soc. **A**, 2293 (1971).
[47] Pauling, L., Z. Krist **69**, 35 (1928).
[48] Pistorius, C. W. F. T., and Admiraal, L. J., Nature **201**, 1321 (1964).
[49] Pistorius, C. W. F. T., Nature **204**, 467 (1964).
[50] Pistorius, C. W. F. T., J. Phys. Chem. Solids **25**, 1477 (1964).
[51] Pistorius, C. W. F. T., J. Chem. Phys. **43**, 1557 (1965).
[52] Pistorius, C. W. F. T., J. Phys. Chem. Solids **26**, 1003 (1965).
[53] Plendl, J. N., and Gielisse, P. J. M., physica stat. sol. **35**, K151 (1969).
[54] Petrunina, T. I., and Estrin, E. I., Dokl. Acad. Nauk. S.S.S.R. **183**, 817 (1968).
[55] Popov, M. M., Simanov, V. P., Skuratov, S. M., and Suzdal'tseva, M. N., Ann. Sect. anal. phys. chim. Inst. Chim. gen. (U.S.S.R.), **16**, 111 (1943).
[56] Pöyhonen, J., and Mansikka, K., phys. Kondens. Materie **3**, 218 (1965).
[57] Pöyhonen, J., Jaakkola, S., and Rasanen, V., Ann. Univ. Turku, Ser. AI **80**, 12 (1964).
[58] Pöyhonen, J., and Ruuskanen, A., Ann. Acad. Sci. Fennicae. Ser. A VI **146**, 12 (1964).
[59] Rao, K. J., and Rao, C. N. R., J. Materials Sci. **1**, 238 (1966).
[60] Rao, K. J., Rao, G. V. S., and Rao, C. N. R., Trans. Faraday Soc. **63**, 1013 (1967).
[61] Rao, K. J., and Rao, C. N. R., Proc. Phys. Soc. (London) **91**, 754 (1967).
[62] Rao, K. J., Rao, G. V. S., and Rao, C. N. R., J. Phys. C. (Proc. Phys. Soc.) **1**, 1134 (1968).
[63] Schulz, L. G., J. Chem. Phys. **18**, 996 (1950); ibid. **19**, 504 (1951).
[64] Schumacher, D. P., Phys. Rev. **126**, 1679 (1962).
[65] Sharma, M. N., and Madan, M. P., Ind. J. Phys. **38**, 231 (1964).
[66] Slykhouse, T. E., and Drickamer, H. G., Coll. intern. centre. natl. recherche, Sci. **77**, 163 (1959).
[67] Smits, A., Z. physik. Chem. **B51**, 1 (1941).
[68] Tosi, M. P., and Fumi, F. G., J. Phys. Chem. Solids **23**, 359 (1962).
[69] Tosi, M. P., J. Phys. Chem. Solids **24**, 1067 (1963).
[70] Tremmel, J., and Morlin, Z., Radex Rundsch., 449 (1967).
[71] Wagner, G., and Lippert, L., Z. Physik chem. **B31**, 263 (1936).
[72] Weijma, H., and Arends, J., phys. stat. solidi **35**, 205 (1969).
[73] Weir, C. E., and Piermarini, G. J., J. Res. Nat. Bur. Stand. (U.S.) **68A** (Phys. and Chem.), No. 1, 105 (1964).
[74] Wood, L. J., Secunda, W., and McBride, H., J. Am. Chem. Soc. **80**, 307 (1958).
[75] Wood, L. J., Sweeney, Ch., and Derbes, M. T., J. Am. Chem. Soc. **81**, 6148 (1959).

3. Ammonium Halides

Phase transitions in ammonium halides as well as their deuterium analogues are well documented in the literature. A wide variety of experimental methods have been employed to study these transitions. While a higher order λ-transition at low temperatures is common to all the halides, a Pm3m(CsCl)-Fm3m (NaCl) transition is exhibited by ammonium chlorides, bromides and iodides and their deuterated analogues at higher temperatures. The latter is a first order transition and is accompanied by considerable thermal hysteresis. In addition to the λ- and Pm3m-Fm3m transitions, a third transition is reported in NH_4Br at ~ 100 K. The λ-transitions of ammonium halides are associated with a change in the rotational motion of the NH_4^+ ion about the ternary axis. Pressure transitions in NH_4X have been reported. Lattice energies of all the four ammonium halides have been estimated theoretically [38] and the calculated values are in good agreement with the observed values.

Much of the theoretical work has been devoted to the λ-transitions in ammonium halides. These λ-transitions are believed to be due to the onset of NH_4^+ ion rotation by Pauling [28a]. While the λ-changes in NH_4Cl and NH_4Br have been attributed to an order-disorder change in the NH_4^+ ion orientation [8a, 25], a temperature-dependent one-dimensional free rotation has been suggested in the case of NH_4I [30]. The low temperature phase of NH_4Cl consists of parallel oriented NH_4^+ groups while the high temperature phase is characterized by randomly oriented NH_4^+ groups [27]. In NH_4Br, the low temperature phase consists of an antiparallel orientation of NH_4^+ ions and the high temperature phase is similar to that of NH_4Cl [26]. Neutron diffraction studies [22, 25] have confirmed the NH_4^+ ion orientations in these halides. The polarization effect of the halide ions is considered to be responsible for the difference in the NH_4^+ ion orientation in the low temperature phases of NH_4Cl and NH_4Br [26]. NMR [10a, 15] and IR [36, 54] studies have been employed to investigate the problem of NH_4^+ ion rotation. Sonin [40] has discussed the possible antiferroelectricity in NH_4I and NH_4Br from a correlation of physical properties with structure.

The Pippard equations and the phase diagram for NH_4Cl have been analyzed in terms of a compressible Ising model; the Pippard relations are completely consistent with the occurrence of a first-order transition in the immediate vicinity of a λ-point [33]. Anomalous heat capacity variations in ammonium halides at low temperatures have been ascribed to second order phase transitions [53]. However, calculations based on available data show that the behavior is described by the Clausius-Clapeyron equation for the first order transitions rather than Ehrenfest's equation for the second order transitions. An abrupt change in dielectric constant at the transition points also indicate a first order transition. A compressible Ising model has also been employed to show that the anomalous ΔV due to ordering is essentially identical with the anomalous changes in the elastic constant, C_{44} [9, 9a].

Thermal Transitions. Ammonium fluoride is hexagonal at room temperature and belongs to B4 group (similar to hexagonal AgI or wurtzite type); this is the only ammonium halide which exists in the hexagonal structure. No transition is known in NH_4F above 298 K. However, a λ-transition at 242 K and a pressure transition around 4000 atm have been reported.

Below 450 K, ammonium chloride possesses the B2 structure with the Pm3m (CsCl type) space group. Phase transitions in NH_4Cl have been the subject of detailed investigation by many workers. The following is the sequence of phase transitions in ammonium chloride.

$$\underset{(Pm3m)}{III} \xleftrightarrow{\sim 240\ K} \underset{(Pm3m)}{II} \xleftrightarrow{\sim 456\ K} \underset{(Fm3m)}{I} \xleftrightarrow{fusion} \underset{NH_4Cl}{liquid}$$

Forms III and II are both CsCl type structures, the transition between them being of λ-type. Form I is of NaCl type (Fm3m) with $a = 6.520$ Å at 523 K. Thus the phase transition at 456 K is a Pm3m-Fm3m transformation similar to the transition in CsCl. The Pm3m-Fm3m transition is of first order and is associated with considerable thermal hysteresis. IR, Raman and NMR spectroscopy, x-ray diffraction, DTA as well as measurements of piezoelectricity, dielectric constant, heat capacity and heat of solution have been employed for the study of the transitions.

Ammonium bromide is body centered cubic (Pm3m, CsCl type) below 411 K. Above this temperature, the structure is face-centered cubic (Fm3m, NaCl type). Just as in NH_4Cl, there are two transitions in NH_4Br. The Pm3m-Fm3m transition takes place at ~ 411 K with appreciable volume change and thermal hysteresis. The transition has been found to be first order. The λ-change takes place around 235 K. In addition to these two transitions a third transition at ~ 102 K has also been reported. The transitions at 235 K and 102 K are also accompanied by hysteresis effects; these transitions have been attributed to changes in the NH_4^+ ion orientation in III and IV phases.

$$\underset{(Pm3m)}{IV} \xleftrightarrow{102\ K} \underset{\substack{Tetragonal\\ (nearly\\ CsCl\ type)}}{III} \xleftrightarrow{235\ K\ \lambda\text{-change}} \underset{(Pm3m)}{II} \xleftrightarrow{411\ K} \underset{(Fm3m)}{I} \xleftrightarrow{fusion} \underset{NH_4Br}{liquid}$$

The room temperature structure of NH_4I is Fm3m. This transforms to the Pm3m structure (CsCl type) at about 257 K. A λ-transition in NH_4I takes place at ~231.3 K. It is interesting to note that the stability range of phase II (CsCl-type) is narrowed down to 25°.

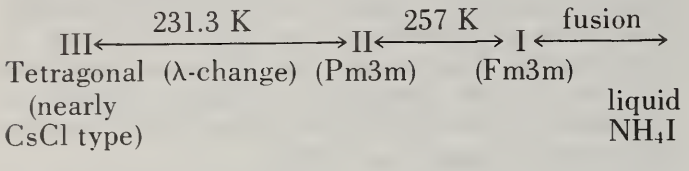

Deuteroammonium halides, ND_4X, exhibit the Pm3m-Fm3m phase transitions with the exception of ND_4I. But a λ-transition is common to all of them just as in their hydrogen counterparts. The Pm3m-Fm3m transitions retain their first-order characteristics in the deuterated solids. The transition temperatures of ND_4X are generally lower than in the corresponding NH_4X, except the III–IV transition of ND_4Br.

The Pm3m-Fm3m transition in ND_4Cl takes place at 448 K while the λ-change occurs at ~ 250 K. These transition temperatures are lower than the corresponding values in NH_4Cl. While the Pm3m-Fm3m transition is accompanied by considerable hysteresis and volume change, the λ-change has no hysteresis effects.

There are three transitions in ND_4Br corresponding to those in NH_4Br:

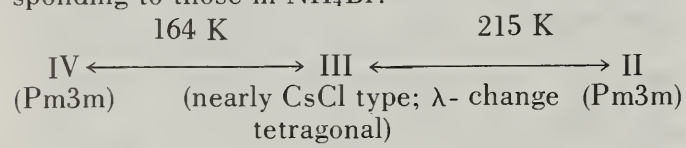

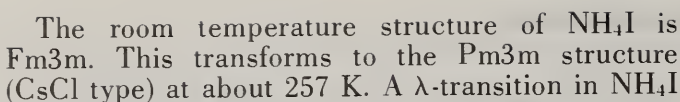

The III–IV transition is faster than in NH_4Br; T_t is also higher in the former case. The ΔV in ND_4Br transitions are comparable to those in NH_4Br.

No literature data seem to be available on ND_4I after Staveley's report [47]. The III–II transition takes place at ~ 229 K, with no thermal hysteresis and negligible volume change (~ −0.1 $cm^3\ mol^{-1}$). This is likely to be a higher order transformation.

Pressure Transitions. Pressure transitions in ammonium halides are not reported extensively in the literature, compared to thermal transitions. The earliest work on pressure-temperature relationships in ammonium halides seems to be that of Bridgman [7a] who reported data for NH_4Cl, NH_4Br and NH_4I between 273 K and 473 K and 12,000 kg cm^{-2}. The only reports on the transition of NH_4F (at ~ 3800 atm and liquid nitrogen temperatures) are that of Stevenson [48], and Swenson and Tedeschi [50a]. Stevenson [49] also reports data on NH_4Cl, NH_4Br, NH_4I and ND_4Br. Adams and Davis [1] report four polymorphic forms for NH_4I. Pressure effects on the λ-transition of NH_4Cl have been investigated by Klynev [17] as well as Trappeniers and co-workers [52]. A systematic investigation of pressure transitions in ammonium halides has been carried out by Pistorius [29] recently. A brief account of phase transitions in ammonium halides has been reported recently by Hovi [11a]. This review summarizes the experimental results from dialatometric, x-ray, calorimetric and NMR studies; the effect of deuteration of ammonium halides is also included.

Ammonium Halides

Substances and measurement techniques	Data	Remarks	References
Ammonium fluoride, NH_4F (P6mc, $a = 4.44$ Å and $c = 7.17$ Å at 298 K)			
Dielectric constant as a function of temperature.	Anomaly in ϵ at ~ 242 K. T_t ~ 241.5 K.	The anomaly in ϵ is due to the λ-transition in NH_4F.	[16].
Ammonium chloride, NH_4Cl (Pm3m, $a = 3.8756$ Å at 299 K)			
	Pm3m-Fm3m transition		
X-ray diffraction	$a_{Pm3m} = 3.868$ Å at 291 K $a_{Fm3m} = 6.52$ Å at 523 K T_t ~ 457.3 K.	Changes of volume, densities accompanying the transition are listed.	[46a].
Specific heat as a function of temperature	T_t ~ 456.1 K, ΔH_{tr} ~ 1030 cal · mol^{-1}	Transition is indicated by an anomaly in the $C_p(T)$ curves.	[6, 37, 55a].

Substances and measurement techniques	Data	Remarks	References
Thermal analysis	$T_t \sim 458$ K; $\Delta H_{tr} \sim 1073$ cal · mol^{-1}. T 8 13.25,; ΔV 8 7.14 cm^3 mol^{-1}.	Hysteresis is shown as a difference in the T_t in heating and cooling curves.	[32a, 37, 42, 57].
Differential Calorimetry	$T_t \sim 456.1$ K; $\Delta H_{tr} \sim 1073$ cal · mol^{-1}.	A detailed discussion of the possible sources of error and their corrections in evaluating the ΔH_{tr} is furnished. The data are likely to be the best for NH_4Cl transition and very reliable.	[2].
Dielectric constant as a function of temperature	$T_t \sim 458$ K.	For single crystals ϵ is 7.08 at 293 K and 2 MHz.	[16].
Dilatometric studies	$T_t \sim 456.1$ K; $\Delta V \sim 19.31\%$ at $T_t \cdot (dT_t/dP) = 0.0724°$ atm^{-1}.	These results compare well with the results of other investigations. The transition conforms to first order as indicated by Clausius-Clapeyron equation.	[31].
Review articles	$T_t \sim 456$ K $\Delta S_{tr} \sim 2.2$ cal deg^{-1} · mol^{-1} ΔV 8 5.26 cm^3 · mol^{-1}.		[11a, 24, 47, 52a].
	λ-transition		
X-ray diffraction down to 80 K	$T_\lambda \sim 243$ K $a = 3.82$ Å at 88 K.		[46, 46a].
Thermal analysis	$T_\lambda \sim 242.5$ K.	The transition is due to a change in the rotational motion of NH_4^+ ion. Hysteresis effects are observed in the transition.	[18, 19].
Differential calorimetry	$T_\lambda \sim 242.1$ K $\Delta T \sim 0.3°$ $\Delta H \sim 109$ cal · mol^{-1}.		[4].
Dielectric constant as a function of temperature	$T_\lambda \sim 242.5$ K.	Transition is indicated by an anomaly in ϵ (T) curve.	[16].
Dilatometric studies; with CBr_4 as the dilatometric liquid.	$\frac{dV}{dT}$ is maximum at $T_\lambda \sim 242.4$ K $\Delta T \sim 0.30°$.	Hysteresis was about 1° if CBr_4 was used.	[43, 51].
Thermal expansion of NH_4Cl and x-ray investigation.	α is maximum between (T_λ), 242 and 242.5 K.	Transition is believed to be due to an order-disorder change.	[7].
Temperature dependence studies of proton and deuteron spin-lattice relaxation in NH_4Cl.	$T_\lambda \sim 242.8$ K; the temperature trend of the nuclear correlation time τ_c is in qualitative agreement with volume-temperature dependence.	There appears to be an indirect relation between the temperature dependence of τ_c and the degree of order in the crystal lattice in the region of the λ-transition.	[58a].
ESR and DTA studies on doped NH_4Cl samples containing a paramagnetic ion, like Cu^{+2}, Ni^{+2} or VO_2^+	T_λ is indicated by a peak in DTA; in ESR, T_λ is indicated where the first derivative of the hyperfine constant with respect to temperature is a maximum.	With increasing Cu^{+2} ion, T_λ decreases. The intensity of the signal in VO_2^+ doped NH_4Cl vanishes at $T_\lambda \sim 241$ K. In the electronic absorption spectrum of Ni^{+2} doped NH_4Cl, a blue shift of 100–150 cm^{-1} observed at ~ 235 K in the positions of the band maxima is attributed to the anomalous lattice contraction of the NH_4Cl lattice.	[20, 28, 35].

Substances and measurement techniques	Data	Remarks	References
Vibrational spectra of thin non-scattering films of NH_4Cl at 301, 195 and 83 K.	No indication of fine structure due to free rotation of the NH_4^+ ion was found. Evidence for the presence of a torsional lattice mode involving the NH_4^+ ions both above and below T_λ was found.	Low temperature modification belongs to T_d' sym. is which the NH_4^+ ion symmetry is T_d. Transition is probably of the order-disorder type.	[56].
Total scattering cross section per H atom measured as a function of temperature by using sub-thermal neutrons.	An apparent change in cross section is observed at T_λ.	The transition involves a change in the rotational motion of the NH_4^+ ion from torsional oscillation to relatively free rotation.	[23].
Review articles	T_t, 247.2 K; $\Delta S \sim 0.82$ eu. $\Delta V \sim 0.16$ cm^3 mol^{-1}.		[11a, 24, 47, 52a].
Ammonium bromide, NH_4Br (Pm3m, $a = 4.059$ Å at 299 K)			
	Pm3m-Fm3m transition		
X-ray diffraction of NH_4Br from 293 to 467 K.	The lattice constants are: $a_I = 6.85187 + 1.38 \times 10^{-5}\, t + 5.385 \times 10^{-7}\, t^2$ $a_{II} = 4.5409 + 2.116 \times 10^{-5}\, t + 3.29 \times 10^{-7}\, t^2$ where t is in °C. $\Delta V_{I \rightarrow II} = 0.0767$ cm$^3 g^{-1}$.	ΔV calculated from x-ray data shows good agreement with the value from dilatometric studies.	[32, 46a].
Solubility as a function of temperature by a close tube method.	$T_t \sim 410$ K	The T_t is indicated by the point of cross section of the solubility curves of I and II phases.	[41].
Dielectric constant as a function of temperature.	$T_t \sim 410$ K	For single crystal NH_4Br, $\epsilon = 7.24$ at 293 K and 2 MHz.	[16].
Thermal analysis	$T_t \sim 410.4$ K; $\Delta T \sim 24°$ $\Delta H_{tr} \sim 882$ cal · mol^{-1} $\Delta V \sim 9.5$ cm^3 mol^{-1}.		[33a, 37, 57].
Dilatometric method (Kinetics of the transition, of NH_4Br at 410.2 K).	$T_t \sim 410.2$ K $\Delta V \sim 18.85\%$ $\left(\frac{dT_t}{dP}\right)$ 0.0878° atm^{-1}. E_a for the transition is ~ 15000 cal · mol^{-1}.	Total volume changes, variation of density and thermal expansion coefficients are discussed. A discussion of thermal expansion behavior is given.	[8, 31].
Rate of transition of supercooled high-temperature modification (NaCl type) of NH_4Br crystallizing from highly supersaturated aqueous solution into the low temperature CsCl phase (by oscillographic recording of the photocurrent change accompanying the I → II transition).	The transition rate is very high and comparable to the speed of sound.	It is inferred that the transition has a martensite character.	[21].

Substances and measurement techniques	Data	Remarks	References
Measurement of specific volumes by hydrostatic weighing in 293–413 K range.	$\Delta V \sim 7.4866$ cm^3 mol^{-1} at T_t for NH_4Br $\Delta V \sim 7.4704$ cm^3 mol^{-1} at T_t (392.5 K) for ND_4Br.	Effect of deuteration of NH_4Br is discussed; ΔV values from the literature are compared and discussed.	[15a].
IR spectra of NH_4Br thin and nonscattering films at 301, 105 and 83 K.	The spectra in phase II is in agreement with the symmetry, D_{4h}. No evidence for free rotation at any temperature is found.		[56].
Review articles	$T_t \sim 414$ K $\Delta V \sim 6.34$ cm^3 mol^{-1}.	Review of phase changes in NH_4Br upto 1964.	[11a, 24, 47, 52a].
	λ-transition		
X-ray diffraction between 295 and 148 K.	For phase II, $a_i = 4.0534 + 1.6 \times 10^{-4}\ t$ (where $i = 1, 2, 3$) $a_i = 4.0539 + 1.34 \times 10^{-4}\ t$ (where $i = 1, 2$) where t is in °C. For Phase III, $a_3 = 4.0537 - 2.72 \times 10^{-4}\ t$ $\bar{V}$, the molar volume (in cm^3 mol^{-1}) is given by $V = 40.113 + 4.82 \times 10^{-3}\ t$ for phase II $V = 40.042 - 2.34 \times 10^{-3}\ t - 3.64 \times 10^{-5}\ t^2$ for phase III. Thermal expansion coefficient, $\alpha = 1.24 \times 10^{-4}$ for phase II $\alpha = -6.0 \times 10^{-5} - 1.8 \times 10^{-6}\ t^2$ for phase III.	$a_1 = a_2 = a_3$ for phase II $a_1 = a_2 \neq a_3$ for phase III	[12, 46a].
DTA	$T_\lambda \sim 234.9$ K.	Transition is believed to be due to the change in the rotational motion of NH_4^+ ion.	[19].
Dielectric constant as a function of temperature.	$T_\lambda \sim 236$ K.		[16].
Dilatometric methods with toluene as the dilatometric liquid.	$T_\lambda \sim 234$ K.	Transformation is heterogeneous and is accompanied by a small hysteresis.	[44].
Total scattering cross section per H-atom measured as a function employing subthermal neutrons.	T_λ is indicated by a change in the cross section.	Transition is due to a change in motion of the NH_4^+ ion from torsional oscillation to relatively free rotation.	[23].
ESR Investigation of NH_4Br single crystals doped with Cu^{+2} ion through λ-point.	The hyperfine constant shows a maximum at ~238 K.	The maximum change at ~ 238 K is due to the λ-change which occurs at ~ 235 K.	[34].
Review articles	$T_t \sim 234.4$ K $\Delta S \sim 0.34$ e.u $\Delta V \sim -0.16$ cm mol^{-1}	Reviews on phase changes in NH_4Br upto 1964.	[11a, 24, 47, 52a].
Ammonium iodide, NH_4I (Fm3m, $a = 7.2613$ Å at 299 K)			

456-089 O - 72 - 4

Substances and measurement techniques	Data	Remarks	References
	Pm3m-Fm3m transition		
X-ray diffraction.	$T_t \sim 257$ K $\Delta V \sim 16.96\%$ $a = 7.259$ Å at 295 K (Fm3m) $a = 4.334$ Å at 252 K (Pm3m)	Effect of particle size on the time for half-conversion in the transition is investigated. Below T_t, the needed super-cooling increases with decreasing particle size.	[12a, 13, 46a].
Differential calorimetry	$T_t \sim 257$ K $\Delta H_{tr} \sim 809$ cal · mol^{-1}	The method is applied for the first time for the study of a transition below 273 K.	[3].
Thermal analysis	$T_t \sim 253$ to 259 K.	Moisture affects the T_t.	[37].
IR investigation of NH_4I in phase I.	$T_t \sim 255.4$ K.	In phase I, one hydrogen bond is formed with I^- and the NH_4^+ ion rotates freely about this bond.	[30].
Review articles	$T_t \sim 258$ K $\Delta V \sim 8.14$ cm^3 mol^{-1}.	Reviews upto 1964.	[11a, 24, 47, 52a].
	λ-transition		
X-ray diffraction	$a_i = 4.3387 + 2.41 \times 10^{-4} t$ ($i = 1, 2, 3$) ($a_1 = a_2 = a_3$ for phase II) $a_i = 4.3439 + 2.28 \times 10^{-4} t$ ($i = 1, 2$); $a_3 = 4.2999 - 1.071 \times 10^{-3} t - 6.41 \times 10^{-6} t^2$ ($a_1 = a_2 \neq a_3$ for phase III).	Molar volume changes are given as a function of temperature.	[13].
Differential thermal analysis.	$T_\lambda \sim 231.35$ K.	Transition is likely to be associated with a change in the NH_4^+ ion rotation.	[19].
Molar volume as a function of temperature.	$T_\lambda \sim 233$ to 213 K.	Above the T_λ the structure is regular and below T_λ the structure is tetragonal.	[44].
Dielectric constant (ϵ' and ϵ'') measurements.	Two maxima between 253 and 233 K are observed.	The rotation of NH_4^+ ion along the N–H axis cannot explain these maxima.	[16, 24].
Review articles.	$T_\lambda \sim 233$ K $\Delta S \sim 0.3$ eu $\quad \Delta T \approx 0$. $\Delta V \sim -0.1$ cm^3 mol^{-1}.		[11a, 24, 47, 52a].
Deuteroammonium chloride, ND_4Cl (Pm3m, $a = 3.8682$ Å at 291 K)			
X-ray diffraction.	$a_{Pm3m} = 3.8190$ Å at 88 K; $a_{Pm3m} = 3.8682$ Å at 291 K. $T_t \sim 448$ K (for II-I transition). $T_\lambda \sim 249.4$ K.		[7, 46a].
Neutron diffraction.	The nature of the NH_4^+ ion rotation is examined.	The neutron diffraction results are in agreement with spectroscopic results of Wagner and Hornig.	[22].
IR spectra of their non-scattering films at 301.295 and 83 K.	The evidence for the order-disorder nature of the second order transition is confirmed.	No evidence of fine structure due to free rotation of NH_4^+ ion was found. Evidence for the presence of a torsional lattice mode involving the NH_4^+ ion both above and below λ-point was available. Low temperature modification belongs to the T_d' symmetry in which the NH_4^+ ion symmetry is T_d. λ-point transitions are probably order-disorder type.	[56].

Substances and measurement techniques	Data	Remarks	References
Review article.	$T_t \sim 448$ K for Pm3m–Fm3m transition. $T_\lambda \sim 249.3$ K: $\Delta V \sim 0.13$ cm mol^{-1}.		[11a, 47].
Deuteroammonium bromide, ND_4Br (Pm3m, $a=4.06$ Å at 299 K)			
X-ray diffraction.	T_t, I → II ~ 393 K; $\Delta V \sim 7.61$ cm mol^{-1} at 398 K: T_λ, II → III ~ 215 K; $\Delta V \sim -0.293$ cm · mol^{-1} at 215 K. III → IV ~ 164 K; $\Delta V \sim 1.08$ cm · mol^{-1} at 164 K. *Lattice constants* $a=6.889$ Å at 469 K (phase I) $a=4.084$ Å at 385 K (phase II) $a=4.047$ Å, $c=4.062$ Å at 195 K (phase III); $a=4.016$ Å at 152 K (phase IV).	Replacement of H by D lowers the T_t while the volume changes, ΔV, are not very much affected. In ND_4Br some metastable states (with BCC structure) were observed in the range 408–399 K.	[14, 46a].
Neutron diffraction.	The nature of rotation of NH_4^+ ion is examined.	The freely rotating model is not tenable with the experimental results.	[22].
Heat capacity in the range 17 to 300 K.	Two maxima in the C_p versus T curve are noted. The first maxima is associated with the polymorphic transition in the crystal lattice and the second one with the ordering of the NH_4^+ ion tetrahedra with respect to the two equilibrium positions in the unit cell. $T_\lambda \sim 215$ K; $\Delta H_\lambda \sim 307$ cal · mol^{-1}. $T_t \sim 166$ K; $\Delta H_{tr} \sim 340.5$ cal · mol^{-1}. ΔH values are obtained from the integrated areas under the peaks.		[50].
IR spectra of thin nonscattering films of ND_4Br at 301, 95 and 83 K.	The symmetry of ND_4Br in Phase III is D_{3h}^1, in accordance with x-ray data.	No evidence for free rotation at any temperature studied, was found. Below 173 K, ND_4Br transforms to phase IV where the symmetry is T_d just as in NH_4Cl.	[56].
Spin-lattice relaxation and phase transition in ND_4Br, at 163.9 K.	In 99 percent of the sample, a hysteresis effect was observed. With a 94 percent ND_4Br no such hysteresis effect was observed.	Assuming the activation energy for the transition to be a function only of the lattice type, the behavior of 99% ND_4Br can be explained in terms of coexistence of two phases at 163.9 K.	[58b].
Neutron diffraction study of the NaCl phase.	Four different models are considered to explain the experimentally observed phenomena of transition.	The freely rotating ND_4^+ ion model is not tenable, with the observed experimental situation. IR absorption data on thin films by Wagner and Hornig support a model involving a single-axis rotation of NH_4^+ ion.	[22].
Review articles.	$T_t \sim 405$ K (Pm3m-Fm3m) $T_\lambda \sim 215$ K; $\Delta V \sim -0.17$ cm mol^{-1}, $\Delta T \sim 0.06°$.		[11a, 24, 47].

Substances and measurement techniques	Data	Remarks	References
Pressure Transitions of Ammonium Halides			
Pressure transition in NH_4F.	$P_T \sim 3800$ atmospheres at room temperature; volume change is 28%. The high pressure phase is FCC at this pressure. With still high pressures of ~ 11 kbar a BCC phase is obtained where the volume change is ~ 11% of the zero pressure volume.	The phase change occurs at a very high pressure at liquid nitrogen temperature. The recovery begins only when the pressure is completely removed. The phase change involves a collapse of the wurtzite structure into a cubic modification.	[48, 50a].
X-ray investigation of high pressure phases of NH_4F and ND_4F, under purely hydrostatic conditions.	The high pressure phase in both the cases is likely to be tetragonal. The transitions are observed at 3.64 $\pm$0.02 kbar in both fluorides.		[24a].
DTA study of pressure effects on λ-transition in NH_4Cl and ND_4Cl up to 2700 atmospheres.	Transition entropy and enthalpy decrease up to 1500 atmospheres and remain unchanged thereafter.	The fact that the entropy of transition is reduced by increased pressure, cannot be explained on the basis of an order-disorder theory which pictures the transition as due to a reorientation of NH_4^+ ion over two sites ($\Delta S = R \ln 2$).	[52].
Spectral investigation of the λ-transition in NH_4Cl up to 23 kbar pressure in the range 3000–7000 cm^{-1}.	The λ-transition takes place around 13–15 kbar at room temperature. The transition was followed by noticing the change of the absorption band with pressure.	The change is associated with the suppression of the random orientation of the NH_4^+ ions, in the crystal lattice. Lattice vibration frequencies are affected to a greater extent than the intramolecular vibration frequencies by pressure.	[17].
Ultrasonic investigation of the high pressure transition in NH_4Br single crystals.	The adiabatic elastic constants of NH_4Br crystals have been measured at 200 MHz as a function of temperature and pressure in the ranges 180–240 K and 0–6 kbar. A new high pressure ordered phase designated as 0_{II} was noticed in this range.	The behavior of NH_4Br is compared with that of NH_4Cl near its order-disorder phase transition.	[10].
DTA of ammonium halides up to 40 kbar; the pressure-temperature curves of the halides are given.	NH_4F has a triple point at 16.8 kbar and 582 K. The melting curve of NH_4F shows an increase up to 706 K at 40 kbar.	The λ-changes in NH_4Cl and ND_4Cl possibly change to first order transitions above 30 kbar.	[29].
Volumetric study of the pressure transitions in NH_4Cl and NH_4Br up to 12000 Kg cm^{-2} between 273 K and 473 K.	$\Delta H_{tr} \sim 100$ cal · mol^{-1}(NH_4Cl). $\Delta H_{tr} \sim 160$ cal · mol^{-1}(NH_4Br).	The ΔH_{tr} in NH_4Cl is independent of pressure. These anomalies may in part be explained with Pauling's suggestion that there is a change from torsional oscillation to rotational motion of NH_4^+ ions; further considerations may be necessary to account for the different behaviors of NH_4Cl and NH_4Br.	[7a].

Substances and measurement techniques	Data	Remarks	References
Piston displacement technique down to liquid nitrogen temperatures, on NH_4Cl, NH_4Br, NH_4I and ND_4Cl, ND_4Br and ND_4I.	*Transition temperature, K* $\alpha-\beta$ / $\beta-\gamma$ / $\beta-\delta$ / $\gamma-\delta$ NH_4Cl..... 458 * 243 * ND_4Cl..... – * 249 * NH_4Br..... 411 235 * 100 ND_4Br..... 398 215 * 169 NH_4I..... 257 231 * * ND_4I..... 254 227 * * *No transition takes place at atmospheric pressures.	The Ammonium tetrahedra are placed on the face of the cube as in the α-phase or at the center of the cube for all the other phases. In β-, γ-, and δ-phases the NH_4^+ tetrahedra are located at the center of the cube formed by the halide ions. The tetrahedra are oriented in a parallel sense in δ-phase from cell to cell; in γ-phase there is antiparallel orientation while in the β-phase the orientation is randomly.	[49].
Modified Bridgman's device with diamond and beryllium anvils employed to study pressure changes up to 20 kbars, in NH_4I.	NH_4I which exists in Fm3m structure at room temperature changes to Pm3m at ~500 bars.	The transition conforms to first order at the start but second order effects are prominent during the major interval of the change.	[1].

References

[1] Adams, L. H., and Davis, B. L., Am. J. Sci. **263**, 359 (1965).
[2] Arell, A., Ann. Acad. Fennicae. Ser. A VI **57** (1960).
[3] Arell, A., and Alare, O., Phys. Kondens. Materie **2**, 423 (1964).
[4] Arell, A., Ann. Acad. Fennicae, Ser. A VI **204**, 5 (1966).
[5] Ayant, Y., and Soutif, M., Compt. rend. **232**, 639 (1951).
[6] Birge, P., and G. Blanc, J. Phys. Radium **21**, Suppl. 141A–145A (1960).
[7] Boiko, A. A., Kristallografiya **14**, 639 (1969).
[7a] Bridgman, P. W., Phys. Rev. **38**, 182 (1931).
[7b] Crystal Data, ACA Monograph. No. 5. Eds. J. D. H. Donnay and G. Donnay, American Crystallographic Association (1963).
[8] Erofeev, B. V., and Mendeleev, L. T., Vesti. Akad. Navuk. Belarus. S.S.R. Ser. Fiz. Tech. Navuk 57 (1957).
[8a] Frenkel, J., Acta. Physicochim. U.R.S.S. **3**, 23 (1935).
[9] Garland, C. W., and Young, R. A., J. Chem. Phys. **48**, 146 (1968).
[9a] Garland, C. W., and Jones, J. S., Bull. Am. Phys. Soc. Ser. 2, **8**, 354 (1963).
[10] Garland, C. W., and Robert, R. A., J. Chem. Phys. **49**, 5282 (1968).
[10a] Gutoswsky, H. S., Pake, G. E., and Bersohn, R., J. Chem. Phys. **22**, 643 (1954).
[11] Hovi, V., and Varteva, M., Phys. Kondens. Materie **3**, 305 (1964).
[11a] Hovi, V., Proc. Intern Conf. Sci & Tech. of Non-metallic Crystals (New Delhi India) (1969).
[12] Hovi, V., Heiskanen, K., and Varteva, M., Ann. Acad. Sci. Fennicae, Ser. A. **144**, 12 (1964).
[12a] Hovi, V., Paavola, K., and Nurmi, E., Ann. Acad. Sci. Fennicae **A, 328** (1969).
[13] Hovi, V., and Lainio, J., Ann. Acad. Sci. Fennicae. Ser. A, **215**, 1 (1966).
[14] Hovi, V., Paavola, K., and Urvas, O., Helv. Phys. Acta. **41**, 938 (1968); Ann. Acad. Sci. Fennicae, Ser. A. **291** (1968).
[15] Itoh, J., Kusaka, R., and Saito, Y., J. Phys. Soc. (Japan), **17**, 463 (1962).
[15a] Jaakkola, S., Pöyhonen, J., and Simola, K: Ann. Acad. Sci. Fennicae, **A, 295** (1968).
[16] Kamiyoshi, K; Sci. Repts, **A8**, 252 (1956).
[17] Klynev, Yu. A., Soviet Physics—Solid State **8**, 322 (1966).
[18] Klug, H. P., Northwest Sci. **10**, 13 (1936); **11**, 36 (1937).
[19] Klug, H. P., and Johnson, W. W., J. Am. Chem. Soc. **59**, 2061 (1937).
[20] Kuroda, N., Kawamori, A., and Mito, E., J. Phys. Soc. (Japan), **26**, 868 (1969).
[21] Kuzmin, S. V., Rab. Fiz. Tverd. Tela **2**, 155 (1967).
[22] Levy, H. A., and Peterson, L. W., J. Chem. Phys. **21**, 366 (1953); Phys. Rev. **83**, 1270 (1951); **86**, 766 (1952).
[23] Leung, P. S., Taylor, T. I., and Havens, W. W., Jr., J. Chem. Phys. **48**, 4912 (1968).
[24] Meinnel, J., Bull. Soc. Sci. Bretagne **39**, 31 (1964).
[24a] Morosin, B., and Shirber, J. E., J. Chem. Phys. **42**, 1389 (1965).
[25] Nagamiya, T., Proc. Phys. Math. Soc. Japan **24**, 137 (1942).
[26] Nagamiya, T., Proc. Phys. Math. Soc. Japan **25**, 540 (1943).
[27] Nagamiya, T., compt. rend. 251 (1952).
[28] Narayana, P. A., and Venkateswarlu, P., J. Chem. Phys. **52**, 5159 (1970).
[28a] Pauling, L., Phys. Rev. **36**, 430 (1930).
[29] Pistorius, C. W. F. T., J. Chem. Phys. **50**, 1436 (1969).
[30] Plumb, R. C., and Hornig, D. F., J. Chem. Phys. **21**, 366 (1953).
[31] Pöyhönen, J., Ann. Acad. Sci. Fennicae. Ser. A. **58**, 52 (1960).
[32] Pöyhönen, J., Mansikka, K., and Heiskanen, K., Ann. Acad. Sci. Fennicae, Ser. A., **168**, 8 (1964).
[32a] Rao, K. J., and Rao, C. N. R., J. Materials. Sci. **1**, 268 (1966).
[33] Renard, R., and Garland, C. W., J. Chem. Phys. **45**, 763 (1966).
[34] Sastry, M. D., and Venkateswarlu, P., Proc. Ind. Acad. Sci. **A66**, 208 (1967).
[35] Sastry, M. D., and Venkateswarlu, P., Molecular Physics **13**, 161 (1967).
[36] Sato, Y., J. Phys. Soc., Japan **20**(12), 2304 (1965).
[37] Scheffer, F. E. C., Proc. Akad. Wetenschappen **18**, 446 (1915); 1498 (1916); Proc. Akad. Sci. Amsterdam, **19**, 798 (1917).
[38] Sharma, M. N., and Madan, M. P., Ind. J. Phys. **38**, 305 (1964).
[39] Shustin, O. A., Yakovlev, I. A., and Velichkina, T. S., JETP Letters **5**, 3 (1967).
[40] Sonin, A. S., Kristallografiya **6**(1), 137 (1961).
[41] Smits, A., and Eastlack, H. E., J. Am. Chem. Soc. **38**, 1261 (1916).
[42] Smits, A., Eastlack, H. E., and Scatchard, G., J. Am. Chem. Soc. **41**, 1961 (1919).
[43] Smits, A., and Mac Gillavry, C. H., Z. physik. Chem. **A166**, 97 (1933).

[44] Smits, A., Ketelaar, J. A. A., and Muller, G. J., Z. physik. Chem. **A175**, 359 (1936).
[45] Smits, A., and Muller, G. J., Z. physik. Chem. **B36**, 140 (1937).
[46] Stammler, M., Orcutt, D., and Colondy, P. C., Advan. X-ray Anal. **6**, 202 (1962).
[46a] Stammler, M., J. Inorg. Nucl. Chem. **29**, 2203 (1967).
[47] Staveley, L. A. K., Quart. Rev. **3**, 64 (1949).
[48] Stevenson, R., J. Chem. Phys. **34**, 346 (1961).
[49] Stevenson, R., J. Chem. Phys. **34**, 1757 (1961).
[50] Stephenson, C. C., and Karo, A. M., J. Chem. Phys. **48**, 104 (1968).
[50a] Swenson, C. A., and Tedeschi, J. R., J. Chem. Phys. **40**, 1141 (1964).
[51] Thomas, D. G., Staveley, L. A. K., and Cullis, A. F., J. Chem. Soc., 1727 (1952).
[52] Trappeniers, N. J., and Van der Molen, Th. J., Physica **32**, 1161 (1966).
[52a] Ubbelohde, A. R., Quart. Rev. **11**, 246 (1957).
[53] Urbakh, V. Yu., Zhur. Fiz. Khim. **30**, 217 (1956).
[54] Vedder, W., U.S. Dept. of Com. Office Tech. Serv. PB Rept., 143–474, 96 p. (1958).
[55] Venkataraman, G., Deniz, K. U., Iyengar, P. K., Roy, A. P., and Vijayaraghavan, P. R., J. Phys. Chem. Solids. **27**, 1103 (1966).
[55a] Voronel, A. V., and Garber, S. R., Zh. Eksp. Teor. Fiz. **52**(6), 1464 (1967)
[56] Wagner, E. L., and Hornig, D. F., J. Chem. Phys. **18**, 296, 305 (1950).
[57] Wallace, R. C., Cent. Min. 33 (1910).
[58] Woessner, D. E., and Snowden, B. S., J. Phys. Chem. **71**(4), 952 (1967); J. Chem. Phys. **47**(7), 2361 (1967).

4. Alkaline Earth (Group IIA) Halides

Substances and measurement techniques	Data	Remarks	Reterences
Beryllium fluoride, BeF_2 (Tetragonal, a=6.60 Å and c=6.74 Å)			
X-ray diffraction and DTA.	Three DTA peaks are observed at 308, 673 and 818 K. The transition at 308 K is a change from tetragonal to cubic structure, with a=6.78 Å; this is an edge centered cubic structure. (8 molecules in the unit cell]. .	The peak at 673 K does not produce any new form. The products after heating in the range 673 to 803 K showed x-ray patterns of cubic form only.	[5, 8a].
High pressure transitions up to 873 K and 60 kbar.	At 773°, BeF_2 transforms from the quartz form to the coesite form, under pressure. At room temperature transition occurs at ~ 15.5 kbar.	Some high pressure phases are also produced by grinding.	[1 to 4].
Beryllium chloride, $BeCl_2$ (orthorhombic, Ibam, a=5.36 Å, b=9.86 Å and c=5.26 Å)			
X-ray diffraction and DTA.	On cooling the melt rapidly, the α' phase is obtained. The structure of α'-$BeCl_2$ is similar to SiS. The α'-phase on heating to 523 K gives a cubic modification (β'). The β' form on further heating to 613 K produces the stable β form. If, however, the melt is allowed to slow equilibrium cooling the α form is encountered at ~ 698 K and further to β form at ~ 678 K.		[6, 9].
Heat capacity in the range 13 to 715 K.	T_t is ~ 676 K for the $\alpha-\beta$ transition; ΔH_{tr} ~ 1495±50 cal mol^{-1}.	Thermodynamic properties for $BeCl_2$ are tabulated for the range 0–750 K.	[8].
Beryllium iodide, BeI_2 (Tetragonal, P4/nmm. a=6.12±0.01 Å and c=10.63±0.04 Å)			
Two forms of BeI_2 are known with a transition at 623 K.	Form I is tetragonal; this transforms to Form II (orthorhombic) above 623 K. The lattice constants of Form II are: a = 16.48 ± 0.02 Å, b=16.702±0.01 Å and c=11.629± ±0.01 Å. $\Delta V \approx 0$.	The number of molecules per unit cell is 4 in the low temperature phase, while there are 32 molecules in the high temperature phase.	[7].

Substances and measurement techniques	Data	Remarks	References
Fluorides of calcium, Magnesium Strontium and Barium			
Changes in lattice spacings of CaF_2. SrF_2. and BaF_2 investigated by x-ray diffraction at pressures up to 65 kbar in a tetrahedral anvil press.	Transitions to structures of lower symmetry take place at ~30 kbar in BaF_2 and at ~60 kbar in SrF_2.	The dependence of the repulsive potential on interionic distances is estimated. Various alternative assignments of repulsive parameters b and ρ for the individual ion-ion interactions are discussed in the light of the Born model. The repulsive parameters appropriate to alkali halides are insufficient to provide the observed repulsion energy.	[10].
X-ray studies up to 160 kbar.	CaF_2 transforms reversibly to α-$PbCl_2$ structure (space group V^{16} Pbnm) around 80 kbars; a=3.50 Å. b=5.64 Å and c=6.96 Å ($\Delta V/V \sim 10\%$). In SrF_2 and BaF_2. the high pressure α-$PbCl_2$ phases could be recovered: in BaF_2. the transition is around 20 kbar. The lattice parameters of the α-$PbCl_2$ phases are: SrF_2: a=3.804 Å; b=6.287 Å; c=7.469 Å; $\Delta V/V \sim 8\%$ BaF_2: a=4.035 Å; b=6.676 Å; c=7.879 Å; $\Delta V/V \sim 11\%$.	MgF_2 reveals no transformation up to 160 kbar.	[2a].

References

[1] Dachille, F., and Roy, R., Z. Krist. **111**, 451 (1959).
[2] Dachille. F., and Roy. R., Nature **186**, 34 (1960).
[2a] Dandekar, D. P., and Jamieson, J. C., personal communication (1971).
[3] Douglas, T. B., STAR, **2**, 1348A (1964).
[4] Kirkina, D. F., Novoselova, A. V., and Simanov, Yu. P., Proc. Akad. Sci., U.S.S.R., Sect. Chem. **107**, 201 (1956).
[5] Kirkina, D. F., Novoselova, A. V., and Simanov, Yu. P., Doklady Akad. Nauk. S.S S.R. **107**, 837 (1956).
[6] Kuvyrkin, O. N., Breusov, O. N., Novoselova, A. V., and Semenenko, K. N., Zhur. Fiz. Khim. **34**, 343 (1960).
[7] Johnson, R. E., Staritzky, E., and Douglass, R. M., J. Am. Chem. Soc. **79**, 2037 (1957).
[8] McDonald, R. A., and Oetting, F. L., J. Phys. Chem. **69** (11), 3839 (1965).
[8a] Novoselova, A. V., and Simanov, Yu. P., Uchenye Zapiski, Moskov Gosudarst. Univ. im. M. V. Lomonosova No. **174**, 7 (1955).
[9] Rundle, R. E., and Lewis, P. H., J. Chem. Phys. **20**, 132 (1952).
[10] Smith, H. I., and Chen, J. H., Bull. Am. Phys. Soc. **11**, 414 (1966).

5. Group IIIA Halides

There are no data available regarding the phase transitions of the halides of boron and gallium. AlF_3 is known to exist in two polymorphic forms, α and β [7a]. NQR investigations have shown that InI_3 undergoes a sluggish transformation under pressure at low temperatures [4a]. There are, however, a few reports on the phase transitions of thallium halides. TlF is orthorhombic [8] and undergoes a phase change at ~354 K to a tetragonal structure [10]. TlCl [5, 9, 15], TlBr [15, 16] and TlI [11] which crystallize in the CsCl structure transform to the NaCl structure when evaporated into thin films on suitable substrates at low temperatures [3, 7, 12, 13]. The abnormal NaCl structures have been examined by electron diffraction as well as x-ray diffraction techniques. Lattice energies of the thallium halides have been calculated by Mayer [8a]. Altshuller [1] as well as Sharma and Madan [14]. No pressure transformation is known in TlCl or TlBr up to 500 kbar [11a]; three high pressure polymorphs of TlF are known [10].

Substances and measurement techniques	Data	Remarks	References
Aluminum fluoride, AlF_3 (Rhombohedral, R32–D_3^7; a=5.039 Å, α=58°31′ at 298 K)			
Heat capacity as a function of temperature.	$T_t \sim 718$ K $\Delta H_{tr} \sim 160$ cal·mol^{-1}.		[7a].
Indium triiodide, InI_3			
NQR investigations and pressure-dependence studies.	The sample changes from normal yellow to brick red color at low temperatures, indicating a sluggish transition, under pressure.	Extrapolation of data seems to suggest that the transition may be feasible around 200 K at atmospheric pressure. Earlier observations indicated a transition around 77 K, at atmospheric pressures.	[4a, 13a].
Thallium fluoride, TlF (orthorhombic D_{2h}^{23}-Fmmm, a=5.495 Å, b=6.08 Å and c=5.18 Å at 298 K)			
X-ray and DTA investigation of high temperature and high pressure transitions.	$T_t \sim 354$ K. The space group of the tetragonal structure (I) is D_{4h}^{17-14}/mmm; a=3.771 Å and c=6.115 Å at 408 K, z=2. A high pressure transition is observed at $\sim$12.6 kbars and 128.5 K. TlF(II) is orthorhombic with D_{2h}^{23}-Fmmm; a=5.18 Å, b=5.495 Å, c=6.08 Å; z=4.	The orthorhombic to tetragonal transition is accompanied by a decrease in density. Pressure-temperature curves of TlCl, TlBr and TlI are also presented.	[10].
Thallium chloride, TlCl (Pm3m, a=3.8427 Å at 298 K)			
Thin films of TlCl evaporated on to amorphous bases at low temperatures and investigated by electron and x-ray diffraction.	Abnormal NaCl structure was observed with a=6.30–6.37 Å around 208 K.	The stability of the NaCl phase is influenced by the base and the temperature.	[3, 7, 12, 13].
Thallium bromide, TlBr (Pm3m, a=3.9588 Å at 298 K)			
Thin films of TlBr evaporated on to amorphous bases and investigated by electron and x-ray diffraction.	a_{Fm3m}=6.58–6.63 Å around 213 K.	The NaCl structure disappears with increase in temperature.	[3, 7, 12, 13].
Thallium iodide, TlI (orthorhombic, D_{2h}^{17}-Cmcm, a=4.582 Å, b=12.92 Å and c=2.251 Å at 298 K)			
Thin layers of TlI evaporated on to amorphous bases (or ionic crystals) and examined by electron and x-ray diffraction.	The CsCl type structure of TlI has a_{Pm3m}=4.205 Å at 288 K. a_{Fm3m}=6.94 Å (on LiF substrate).	The CsCl structure passes onto the orthorhombic structure near room temperature. It is interesting that TlI deposited on LiF has the NaCl structure.	[3, 5a, 7, 12 13].

Substances and measurement techniques	Data	Remarks	References
X-ray and DTA investigation; pressure transition in TlI.	TlI transforms from a layer orthorhombic to cubic structure at 430 K. $\Delta H_{tr} \sim 293 \pm 38$ cal · mol^{-1} (from DTA) ~ 321 cal · mol^{-1} (from Clausius-Clapeyron equation). $a_0 \sim 4.2099$ Å at 293 K for the high temperature form (extrapolated) P_T 4.7±0.1 kbar at 298 K. $\Delta V \sim 3.3\%$ at P_T. α shows in the range 296–443 K. $\alpha_a = 15.90 \pm 0.5 \times 10^{-6}$ (°C)$^{-1}$ $\alpha_b = 48.7 \pm 0.3 \times 10^{-6}$ (°C)$^{-1}$ $\alpha_c = 60.4 \pm 0.6 \times 10^{-6}$ (°C)$^{-1}$. For the cubic phase, $\alpha_a = 51.0 \pm 0.3 \times 10^{-6}$ (°C)$^{-1}$, between 443–573 K.	The transition at 430 K is also accompanied by about 35% change in dielectric constant ϵ. Structural and thermodynamic aspects of the transition are discussed.	[4, 11, 17].
Dilatometric study.	$T_t \sim 423$–447 K $\Delta V \sim 0.003$ cm^3 g^{-1}.	The transition is autocatalytic. Presence of gases like CO_2, nitrogen or air does not affect the rate of transition.	[2, 6].

References

[1] Altshuller, A. P., J. Chem. Phys. **22**, 1136 (1954).
[2] Benton, A. F., and Cool, R. D., J. Phys. Chem. **35**, 1762 (1931).
[3] Blackman, M., and Kahn, I. H., Proc. Phys. Soc. **77**, 471 (1961).
[4] Bradley, R. S., Grace, J. D., and Munro, D. C., Z. Krist. **120**, 349 (1964).
[4a] Brooker, H. R., and Scott, T. A., J. Chem. Phys. **41**, 475 (1964).
[5] Hambling, P. G., Acta. Cryst. **6**, 98 (1953).
[5a] Helmholtz, L., Z. Krist. **95**, 129 (1936).
[6] Ishikawa, F., and Sato, Y., J. Chem. Soc. Japan **55**, 930 (1934).
[7] Kahn, I. H., Proc. Phys. Soc. (London), **76**, 507 (1960).
[7a] Kirk-Othmer, Encyclopedia of Chemical Technology, 2nd Edition, Vol. **9**, p. 529 (John Wiley & Sons., New York, 1966).
[8] Ketelaar, J. A. A., Z. Krist. **92**, 30 (1935).
[8a] Mayer, J. E., J. Chem. Phys. **1**, 327 (1933).
[9] Meyerhoff, V. K., Acta. Cryst. **12**, 330 (1959).
[10] Pistorius, C. W. F. T., and Clark, J. B., Phys. Rev. **173**, 692 (1968).
[11] Samara, G. A., Walters, L. C., and Northrop, D. A., J. Phys. Chem. Solids **28**, 1875 (1967).
[11a] Samara, G. A., and Drickamer, H. G., J. Chem. Phys. **37**, 408 (1962).
[12] Schulz, L. G., J. Chem. Phys. **18**, 996 (1950).
[13] Schulz, L. G., Acta Cryst. **4**, 487 (1951).
[13a] Segel, S. E., and Barnes, R. G., J. Chem. Phys. **25**, 578 (1956).
[14] Sharma, M. N., and Madan, M. P., Ind. J. Phys. **38**, 305 (1964).
[15] Smakula, A., and Kalanajs, J., Phys. Rev. **99**, 1737 (1955).
[16] Westman, S., and Magneli, A., Acta. Chem. Scand. **11**, 1587 (1957).
[17] Zahner, J. C., and Drickamer, H. G., J. Phys. Chem. Solids **11**, 92 (1959).

6. Group IVA Halides

Carbon tetrafluoride exhibits a first order thermal transformation at ~ 76.2 K and atmospheric pressure [6]; the transformation shows no hysteresis. Stewart [21] observed a volume change of about 1.8 cm^3 mol^{-1} at ~ 89 K. The transition temperature for CF_4 observed by Stewart is, however, higher than that mentioned in the previous report. CCl_4 when cooled below its freezing point undergoes a transformation at ~ 225 K [11, 14]; the transition is accompanied by a change from the cubic to the monoclinic structure. The large enthalpy (~ 1080 cal mol^{-1}) suggests the transition to be of first order. CBr_4 exhibits a similar transformation from a cubic to a monoclinic structure [10].

Bridgman [3] observed three solid forms of CCl_4 in the range 253–473 K and up to 12 kbar; Kleiss and co-workers [12] have reported two pressure transitions in CCl_4 at ~ 4 kbar (I–II) and at ~ 7 kbar (II–III). Bridgman [4, 5] reports pressure transitions in CBr_4. SiF_4 undergoes a pressure transition

from a BCC structure to a close-packed structure in the region 5–20 kbar [21]. A pressure transition occurs at ~ 94.3 K in SiF_6 [6]. $SiCl_4$ is reported to undergo a pressure transition by Bridgman [3]. GeI_2 exists in two hexagonal modifications as evidenced by electron diffraction studies on thin films of GeI_2 [1]. Electrical resistance measurements under pressure indicate a polymorphic change in SnI_4 to a metallic state [17]. PbF_2 exists in two modifications [2] while PbI_2 exhibits polytypism [7, 9]. An x-ray study of over 600 crystals of PbI_2 [8] has revealed some important facts for the formulation of a satisfactory theory of polytypism [9]. Phase changes in PbI_2 have been investigated by the Hahn emanation method of following the emanation of the ^{135}Xe from $Pb^{135}I_2$ [15]. The theory of polytypism has been discussed by Schneer [19]; a systematic account of polytypism with literature references is furnished by Verma and Krishna [22].

Group IVA Halides

Substances and measurement techniques	Data	Remarks	References
Carbon tetrafluoride, CF_4			
Calorimetric study	$T_t \sim 76.2$ K	The transition is reversible with negligible hysteresis.	[6].
Piston displacement method for studying high pressure transition in CF_4	Isothermal pressure—volume curves were examined for solid CF_4. A volume change of ~ 1.8 $cm^3\ mol^{-1}$ is consistent with calculated of ~ 2.0 $cm^3\ mol^{-1}$ for the transition.	The transition is a first order one. No crystal structure data are available for the low and high pressure phases of CF_4.	[21].
Carbon tetrachloride, CCl_4 (cubic, $a = 8.34 \pm 0.03$ Å at 238 K)			
X-ray diffraction	Below 225.3 K an ordered monoclinic phase of CCl_4 is reported. $a = 20.3$ Å, $b = 11.6$ Å, $c = 19.9$ Å; $\beta = 111°$; $Z = 32$; $\rho = 1.868$ g cm^{-3}. Above 225.3 K this phase transforms to a hitherto unknown rhombohedral phase stable up to the melting point.	High pressure studies by Weir et al. [23] furnish the following crystal structure data: CCl_4(I) rhombohedral, $a = 14.27$ Å, $\alpha = 90°$; $Z = 21$. CCl_4(II) monoclinic, (C2/C or Cc), $a = 22.1$ Å, $b = 11.05$ Å, $c = 25.0$ Å, $\beta = 114°$; $Z = 32$. CCl_4(III) orthorhombic, ($C222_1$), $a = 11.16$ Å, $b = 14.32$ Å, $c = 5.74$ Å, $Z = 8$.	[17a, 23].
Calorimetric study employing a modified Nernst vacuum calorimeter.	$T_t \sim 224.4$ K; $\Delta H_{tr} \sim 1080$ cal · mol^{-1}.	A suspension of solid CCl_4 in methanol was employed. The T_t of CCl_4 is very sensitive to impurities and hence not useful as a thermometric standard.	[11, 14, 16, 20].
High pressure changes in CCl_4 investigated by employing a diamond high pressure cell.	Two transformations at ~ 4 and ~ 7 kbar are observed.	Observations of the phase changes were made by using a transmitted light polarizing microscope.	[12].
Carbon tetrabromide, CBr_4 (Monoclinic, $a = 21.12$ Å, $b = 12.26$ Å, $c = 24.14$ Å; $\beta = 125°\ 3'$ also $a = 21.12$ Å, $b = 12.26$ Å, $c = 21.05$ Å; $\beta = 110°\ 10'$)			
Heat capacity of CBr_4 in the range 273–333 K.	$T_t \sim 222.13$ K. $\Delta H_{tr} \sim 1594.5$ cal mol^{-1}. $\Delta S_{tr} \sim 1.87$ cal · mol^{-1} deg^{-1}.	Heat capacity data from experiment and theory are employed to show the absence of free rotation in CBr_4 above T_t. There is essentially no change in the molecular motion at the transition point.	[13].
Dilatometric study	The change is from cubic to monoclinic structure.		[18].
Optical investigation of the kinetics of CBr_4 transition in polycrystalline samples.	$T_t \sim 226.1$ K. The activation energy is of the same order of magnitude as the sublimation energy.	Optical crystallographic data for monoclinic CBr_4 are obtained.	[10].

Substances and measurement techniques	Data	Remarks	References
Silicon tetrafluoride, SiF_4 (BCC, $I\bar{4}3m$ or I23, $a=5.42\pm0.01$ Å)			
Pressure changes in the range 97–200 K by x-ray diffraction.	SiF_4 changes to a close-packed structure at high pressures. Two transitions are known, one at ~ 8.2 kbar and another at ~ 10.2 kbar.	The overall lattice of the low pressure phase is molecular rather than ionic.	[21].
Siliconhexafluoride, SiF_6			
Calorimetry.	$T_t \sim 94.3$ K.	Transition is reversible and discontinuous; likely to be a first order transition.	[6].
Germanium diiodide, GeI_2 (hexagonal, $P\bar{3}m1$, $a=4.13$ Å and $c=6.79$ Å)			
Electron diffraction of thin films.	Two hexagonal forms have been identified. Form I with space group, C_{6v}^4; $a=4.17$ Å and $c=33$ Å. Form II with space group, D_{3d}^3; $a=4.17$ Å and $c=20.16$ Å. Z is 2 and 3 in I and II respectively.	The structure of the I and II Forms comprise of four and six-layer stackings of iodine atoms respectively, the germanium atoms lying in the octahedral spaces of these layers.	[1].
Stannic iodide, SnI_4 (cubic, T_h^6–Pa3, $a=12.273$ Å at 299 K)			
Electrical conductivity measurements on SnI_4.	SnI_4 becomes metallic at about 185 kbar as indicated by a sharp decrease in resistance.	The results are in reasonable agreement with extrapolated optical-gap data.	[17].
Lead fluoride, PbF_2 (α-PbF_2, orthorhombic, D_{2h}^{16}-Pnmb, $a=3.899$ Å, $b=6.4421$ Å, $c=7.6514$ Å at 298 K).			
Thermodynamic properties of PbF_2 at high temperatures and x-ray investigation of phase transition.	PbF_2 exists in two modifications α and β. α transforms to β at ~ 473 K. β-PbF_2 is cubic with $a=5.940$ Å at 299 K.	The T_t was determined thermographically. The high temperature cubic form can also be prepared by the action of HF on $PbCO_3$.	[2, 5a].
Lead iodide, PbI_2 (hexagonal D_{3d}^3; $P\bar{3}m1$, $a=4.557$ Å and $c=6.979$ Å at 298 K).			
Polytypism in gelgrown PbI_2.	Growth conditions and various polytypic structures are linked together. Besides the 2H, 4H, 6R, 6H, and 12R polytypes already known, twenty new polytypes have been found.	The small extent to which polytypism has been observed earlier has been interpreted as lending support to Frank's screw dislocation theory. However, the experimental results prove the importance of growth conditions. For various crystal structure data, reference [5a] may be consulted.	[7, 5a, 22].
X-ray study of about 600 crystals of PbI_2.	A satisfactory epitaxial theory of polytypism has been formulated. A new polytype of the largest size, 48R is described.		[8].

References

[1] Avilov, A. S., and Imanov, R. M., Sov. Phys-Cryst. **13**, 52 (1968).

[2] Banashek, E. I., Patsukova, N. N., and Rassonskaya, I. S., Neorg. Khim Acad. Nauk. S.S.S.R. **27**, 223 (1956).

[3] Bridgman, P. W., Phys. Rev. **3**, 153 (1914); *ibid.*, **6**, 1 (1915).

[4] Bridgman, P. W., Proc. Am. Acad. Arts Sci. **52**, 57 (1916).

[5] Bridgman, P. W., Proc. Am. Acad. Arts Sci. **72**, 227 (1938).

[5a] Crystal Data, ACA Monograph, No. 5, Ed. J. D. H. Donnay, and Donnay, G., American Crystallographic Association (1963).

[6] Eucken, A., and Schroder, E., Math-Physik. Klasse, and Donnay, G., Fachgruppe II, **3**, 65 (1938).

[7] Hanoka, J. I., Vedam, K., and Henisch, H. K., J. Phys. Chem. Solids, Suppl. **1**, 369 (1967).
[8] Hanoka, J. I., and Vand, V., J. Appl. Phys. **39**, 5288 (1968).
[9] Hanoka, J. I., Vedam, K., and Henisch, H. K., Crystal Growth, Ed. H. S. Peiser (Pergamon Press, Inc. Oxford, 1967) p. 369.
[10] Hartshorne, N. H., and Swift, P. McL., J. Chem. Soc. 3705 (1955).
[11] Johnston, H. L., and Long, E. A., J. Am. Chem. Soc. **56**, 31 (1934).
[12] Kleiss, R. M., Nourbakhsh, M., and Alder, P. N., J. Materials Sci. **3**, 657 (1968).
[13] Marshall, J. G., Staveley, L. A. K., and Hart, K. R., Trans. Faraday Soc. **52**, 19 (1956).
[14] McCullough, J. C., and Phipps, H. E., J. Am. Chem. Soc. **50**, 2213 (1928).
[15] Narang, V. P., and Yaffe, L., Canadian J. Chem. **46**, 491 (1968).
[16] Phipps, H. E., and Reedy, J. H., J. Phys. Chem. **40**, 89 (1936).
[16a] Post, B., Acta. Cryst. **12**, 349 (1959).
[17] Rigglemann, B. M., and Drickamer, H. G., J. Chem. Phys. **38**, 2721 (1963).
[17a] Rudman, R., and Post, B., Science **154**, 1009 (1966).
[18] Sakovich, G. V., Zhur. Fiz. Khim. **34**, 2808 (1960).
[19] Schneer, C. J., Acta. Cryst. **8**, 279 (1955).
[20] Skau, E. L., and Meier, H. F., J. Am. Chem. Soc., **51**, 3517 (1929).
[21] Stewart, J. W., J. Chem. Phys. **33**, 128 (1960).
[22] Verma, A. R., and Krishna, P., in Polymorphism and Polytypism in Crystals (John Wiley, New York, 1966).
[23] Weir, C. E., Piermarini, G. J., and Block, S., J. Chem. Phys. **50**, 2089 (1969).

7. Group VA Halides

Substances and measurement techniques	Data	Remarks	References
Arsenic triiodide, AsI_3 (Trigonal C_{3i}^2-$R\bar{3}$, $a=7.208$ Å, $c=21.45$ Å at 298 K).			
Polymorphism in AsI_3.	Two polymorphic forms are known. An yellow (metastable accicular) form is obtained by rapid cooling of a hot benzene or toluene solution. On standing, the yellow crystals change to a stable red form. The conversion becomes faster on heating.	No conversion was observed when the samples were carefully dried and stored at room temperature in the absence of air, even after a period of one month.	[3, 4].
Antimony trichloride, $SbCl_3$ *and Antimony tribromide*, $SbBr_3$.			
Investigation of phase changes in the range 273 to 450 K and up to 30 kbar.	Two new forms for each of the halides were noticed. Their phase diagrams are similar.	Study on SbI_3 and BiI_3 showed no transitions in either of them.	[1a].
Bismuth trifluoride, BiF_3 orthorhombic, Pnma, $a=6.563$ Å, $b=7.021$ Å, $c=4.845$ Å at 298 K).			
Polymorphism in BiF_3.	Two other modifications are reported in the literature. An α-form stable up to 473 K is cubic (Fm3m), with $a=5.865\pm0.06$ Å. α-changes to β-form above 473 K.	For various crystal structure data reference 2 must be consulted.	[1, 4a, 5].
Bismuth triiodide, BiI_3 (Trigonal, C_{3i}^2-$R\bar{3}$, $a=7.522$ Å, $c=20.73$ Å at 298 K).			
Two new forms of BiI_3.	Form I, hexagonal, $R\bar{3}$, with $a=7.5$ Å and $c=20.65$ Å. Form II cubic, with $a=20.676$ Å.		[2].

References

[1] Aurivillius, B., and Lindqvist, T., Acta. Chem. Scand. **9**, 1209 (1955).
[1a] Bowles, B. F., Scott, G. J., and Bable, S. E., Jr., J. Chem. Phys. **39**, 831 (1963).
[2] Crystal Data, ACA Monograph, No. 5, Ed. J. D. H. Donnay, and Donnay, G., American Crystallographic Association (1963).
[3] Hass, D., Z. anorg. allgem. chem. **327**, 84 (1964).
[4] Heyworth, D., Phys. Rev. **38**, 351 (1931).
[4a] Kirk-Othmer, Encyclopedia of Chemical Technology, 2nd Edition, Vol. **3**, p. 539 (John Wiley & Sons., New York, 1964).
[5] Zalkin, A., and Templeton, D. H., J. Am. Chem. Soc. **75**, 2453 (1953).

Substances and measurement techniques	Data	Remarks	References
Titanium trichloride, $TiCl_3$ (α-$TiCl_3$, rhombohedral, R_3, $a = b = 6.12$ Å, $c = 17.50$ Å; $\gamma = 120°$)			
X-ray diffraction	$TiCl_4$ on reduction with hydrogen at 1070 to 1173 K gives α-$TiCl_3$; this is bidimensional and belongs to rhombohedral symmetry, R_3. The coordinates of Ti are: 0, 0 1/3; chlorine atoms are at, 1/3, 0, 0.079. $TiCl_4$ on reduction with aluminum alkyls give β-form of $TiCl_3$; this is a linear polymer. This has a hexagonal structure with $a = b = 6.27$ Å, $c = 5.82$ Å. β-form on heating to about ~ 573 K passes on to a new (γ) modification.		[3a, 14].
Chromium chloride, $CrCl_3$ (Monoclinic, C2/m; $a = 5.959$ Å, $b = 10.321$ Å, $c = 6.114$ Å; $\beta = 108.49°$)			
X-ray diffraction and NQR (^{35}Cl) with $CrCl_3$ single crystals.	$T_t \sim 240$ K. The monoclinic structure transforms to a rhombohedral structure with $R\bar{3}$ symmetry; $a = 5.942$ Å, $c = 17.333$ Å.	The transformation seems to be a first order one.	[13].
Ferrous bromide, $FeBr_2$ (hexagonal, $P\bar{3}m1$, $a = 3.74 \pm 0.05$ Å, $c = 6.171$ Å.)			
X-ray diffraction	$FeBr_2$ undergoes a cooperative second-order transformation at ~ 673 K. The high-temperature phase is different from hcp or random-packed-layer structure of the $Cd(OH)_2$ type.	T_t is markedly affected by the presence of moisture in the sample.	[5].
Ferric fluoride, FeF_3 (hexagonal, $R\bar{3}c$, $a = 5.20$ Å, $c = 13.40$ Å at 291 K)			
X-ray diffraction	FeF_3 grown by sublimation of anhydrous crystals has a cubic symmetry. At 683 K, transition to a rhombohedral structure takes place.	For other data on the hexagonal crystal structure, reference should be made to [4a].	[4].

<table>
<tr><th>Substances and measurement techniques</th><th>Data</th><th>Remarks</th><th>References</th></tr>
<tr><td>Manganese fluoride, MnF_2 (Rutile, $P4_2/mnm$, $a = 13.59 \pm 0.05$ Å, $c = 3.3099 \pm 0.05$ Å at 298 K)</td><td></td><td></td><td></td></tr>
<tr><td>X-ray investigation of high pressure transitions up to 160 kbar and at 298 K.</td><td>At 33 ± 4 kbars, MnF_2 (I) (rutile type) transforms to MnF_2 (II) (a distorted CaF_2 type) with $a = b = 5.03$ Å, $c = 5.28$ Å; density, $\rho = 4.62$ g cm^{-3} at 80 kbar. At higher pressures (150 kbar) a third phase, III, is formed ($a = 3.25$ Å, $b = 5.54$ Å, $c = 6.88$ Å; $\rho = 4.98$ g cm^{-3}). A metastable phase, IV, is obtained on removing the pressure.</td><td>A triclinic form of MnF_2 with 1 point group has been mentioned in the literature and referred to in "Crystal Data" [4a]. The lattice constants are: $a = 5.13$ Å, $b = 5.31$ Å, $c = 5.07$ Å, $\alpha = 180° 30'$, $\beta = 119° 35'$ and $\gamma = 88° 33'$, Dandekar and Jamieson [4b] suggest that the rutile phase transforms to a new tetragonal phase which then transforms reversibly to the α-$PbCl_2$ form ($a = 3.323$ Å, $b = 5.560$ Å, $c = 6.454$ Å; $\Delta V/V = 10\%$).</td><td>[1, 4b, 7, 17].</td></tr>
<tr><td>Pressure transitions of CoF_2, NiF_2, and ZnF_2</td><td></td><td></td><td></td></tr>
<tr><td>X-ray investigation of high pressure changes in CoF_2, NiF_2 and ZnF_2 upto 160 kbar at 298 K.</td><td>The phase changes occur from the low pressure rutile phase to the distorted fluorite structure. The lattice constants and densities are given below:
High pressure phase
a, Å; ρ, g cm^{-3}
CoF_2 ..... 4.91; 5.44
NiF_2 ..... 4.84; 5.66
ZnF_2 ..... 4.82; 6.13
Low pressure phase
a, Å; c, Å; ρ, g cm^{-3}
CoF_2 ..... 4.54; 3.32; 4.70
NiF_2 ..... 4.51; 3.30; 4.78
ZnF_2 ..... 4.41; 3.27; 5.40</td><td>These data have been obtained in 130–150 kbar region at 298 K. X-ray diffraction patterns of these fluorides indicate the presence of a mixture of the high and low pressure phases under these conditions. Dandekar and Jamieson [4b] suggest that the initial rutile structure transforms to another tetragonal structure (starting around 30 kbar) with $a = 4.908$ Å and $c = 4.658$ Å (at 25 kbar); release of pressure yields a mixture of the two phases. There is no further change in structure up to 120 kbar.</td><td>[4b, 7].</td></tr>
<tr><td>Copper (I) Chloride CuCl (T_d^2–$F\bar{4}3m$: $a = 5.416$ Å at 299 K)</td><td></td><td></td><td></td></tr>
<tr><td>X-ray powder pattern of CuCl at high temperatures.</td><td>$T_t \sim 683$ K. The low temperature phase of CuCl is FCC (ZnS) with $a = 5.4057$ Å. The high temperature form has the hexagonal structure ($a = 3.91$ Å and $c = 6.42$ Å).</td><td>The high temperature phase may be similar to wurtzite</td><td>[10].</td></tr>
</table>

Substances and measurement techniques	Data	Remarks	References
High pressure phases in CuCl by studying the $P-T$ curves; conductivity and TEP measurements in the 370–670 K and 10–55 kbar.	A phase diagram has been constructed indicating the stability range of various high pressure phases. The stability of phase I is in a small range of 673–683 K and below 5 kbar. Phase II is stable in the range up to 600 K and 40 kbar. Between 40 and 60 kbar a new phase IIa is reported. IV and V are stable above 60 kbar up to 140 kbar and below 673 K.	Phase I is wurtzite type and phase II is zinc blende type structure. DTA diagrams are given for various phases and their mutual transitions.	[2, 16].
Copper (II) chloride, $CuCl_2$ (Monoclinic, I2/m, $a=6.70$ Å, $b=3.30$ Å, $c=6.67$ Å; $\beta=118°\ 23'$)			
X-ray investigation of polymorphism in $CuCl_2$.	There are two polymorphic forms α and β with a $T_t \sim 761$ K.		[8].
Copper (I) bromide, CuBr (T_d^2-F$\bar{4}$3m, $a=5.6905$ Å)			
Calorimetric and x-ray investigation.	γ-CuBr is FCC with $a=5.6794$ Å at 293 K. This is ZnS type and is like CuI. β-CuBr is hexagonal, C_{6v}^4 $a=4.04$ Å, $c=6.58$ Å at ~ 703 K. α-CuBr is BCC and is similar to α-AgI. $a=4.53$ Å at ~ 753 K. $\Delta H_{\gamma-\beta}=1400$ cal · mol^{-1} $\Delta S_{\gamma-\beta}=2.1$ e.u. mol^{-1} $\Delta H_{\beta-\alpha}=700$ cal · mol^{-1} $\Delta S_{\beta-\alpha}=0.9$ e.u. mol^{-1} β and α are only average structures.		[6].
Microcalorimetric studies (employing DTA)	CuBr (obtained from $CuBr_2$ dissociation at ~ 453 K) exhibits the $\gamma \rightarrow \beta \rightarrow \alpha$ transitions by DTA anomalies.	Immediately after the α-form is formed, CuBr starts melting at ~ 770 K.	[9, 18].
Copper (I) iodide, CuI (cubic T_d^2-F$\bar{4}$3m, γ-form, $a=6.0507$ Å)			
DTA and TGA studies on CuI_2 and CuI.	CuI_2 readily loses iodine and transforms to the β form at ~ 648 K and finally to the α form at ~ 785 K. The solid melts at ~ 873 K. α is cubic, β is hexagonal (ZnO type) and γ is of ZnS type structure.		[9, 15].
Investigation of CuI by x-ray diffraction, heat capacity, etc.	T_t, $\gamma \rightarrow \beta$, 642 K $\beta \rightarrow \alpha$, 680 K.	The high temperature forms (β and α) are average structures.	[12].
High pressure polymorphism in CuBr and CuI, by DTA and x-rays.	In CuI, six phases have been reported: α (FCC phase) β (wurtzite) γ (zinc blende) as well as h_1, h_2, and h_3 phases are known. $\gamma \rightarrow h_1$ transition is at 4 kbar, $h_1 \rightarrow h_2$ at 5 kbar and $h_2 \rightarrow h_3$ at ~ 15 kbar. In the case of CuBr, α (BCC), β (wurtzite) and γ (zinc blende) are all stable below 40 kbar and ~ 800 K.	For both CuBr and CuI phase diagrams are given.	[3, 11, 12, 16].

3*d* Transition Metal Halides—Continued

Substances and measurement techniques	Data	Remarks	References
Zinc chloride, $ZnCl_2$			
Dilatometric study	The glass transition temperature was determined by dilatometric and linear expansion coefficient methods.	The rate of crystallization was also measured dilatometrically and results are presented in detail. There are three forms of $ZnCl_2$ known, α, β, and γ. For the various structural data reference should be made to [4a].	[4c].

Polymorphic Phases of Copper Halides

	Designation	Structure	Range of stability
CuCl	I	wurtzite	Between 650–700 K and below 5 kbar.
	II	zinc blende	Below 650 K and ~ 30 kbar.
	III	BCC (similar to α-AgI)	Above 700 K and 10 kbar.
CuBr	I	BCC (similar to α-AgI)	Above 800 K and ~ 10 kbar.
	II	wurtzite	Between 600–700 K and below ~ 8 kbar.
	III	zinc blende	Below 600 K and up to ~ 30 kbar.
CuI	I	FCC (disordered zinc blende)	Between 675–1000 K and up to 30 kbar.
	II	wurtzite	Between 575–675 K and below ~ 5 kbar.
	III	zinc blende	Below 575 K and ~ 12 kbar.
	IV	.....	Below ~600 K and above ~ 10 kbar.
	V	.....	Above 20 kbar and ~ 600 K.
	VI	.....	Above 30 kbar and around 800 K.
	VII	.....	Above 900 K and ~ 10 kbar.

References

[1] Azzaria, L. M., and Dachille, F., J. Phys. Chem. **65**, 88 (1961).
[2] Bradley, R. S., Munro, D. C., and Spencer, P. N., Trans. Faraday Soc., **65**, 1912 (1969).
[3] Bridgman, P. W., Proc. Am. Acad. Arts Sci. **52**, 91 (1916); Proc. Nat. Acad. Sci. **1**, 513 (1915).
[3a] Cras, J. A., Nature **194**, 678 (1962).
[4] Croft, W. J., and Kestigian, M., J. Electrochem. Soc. **115**, 674 (1968).
[4a] Crystal Data, ACA Monograph, No. 5, Ed. J. D. H. Donnay, and Donnay G., American Crystallographic Association (1963).
[4b] Dandekar, D. P., and Jamieson, J. C., personal communication (1971).
[4c] Eisenberg, A., and Hilemen, B. J., U.S. Gov. Res. Rep. **39**, 108A (1964).
[5] Gregory, N. W., and O'Neal, H. E., J. Am. Chem. Soc. **81**, 2649 (1959).
[6] Hoshino, S., J. Phys. Soc. Japan **7**, 560 (1952).
[7] Kabalkina, S. S., Vereshchagin, L. F., and Lityagina, L. M., Sov. Phys. Solid State **11**, 847 (1969).
[8] Korzhukov, N. G., and Psalidas, V. S., Vestn. Mork. Univ. Khim. **23**, 54 (1968).
[9] Le-Van-My, Perinet, G., and Bianco, P., Bull. Soc. Chim. France **12**, 3651 (1965).
[10] Lorenz, M. R., and Prener, J. S., Acta. Cryst. **9**, 538 (1956).
[11] Mao-Chia, Y. W., Schwartz, L. H., and La Mori, P. N., J. Phys. Chem. Solids **29**, 1633 (1968).
[12] Miyake, S., Hoshino, S., and Takenaka, T., J. Phys. Soc. Japan **7**, 19 (1952).
[13] Morrison, B., and Narath, A., J. Chem. Phys. **40**, 1958 (1964).
[14] Natta, G., Corrodini, P., Bassi, I. W., and Porri, L., Atti. acad. nazl. Lincei, Rend. **24**, 121 (1951).
[15] Pechkovskii, V. V., and Sofronova, A. V., Zh. Neorgan. Khim. **10**, 1513 (1965).
[16] Rapoport, E., and Pistorius, C. W. F. T., Phys. Rev. **172**, 838 (1968).
[17] Vereshchagin, L. F., Kabalkina, S. S., and Kotilevets, A. A., Sov. Phys. JETP **22**, 1181 (1966).
[18] Winkler, H. G. F., Z. anorg. u. allgem. chem. **276**, 169 (1954).

9. 4*d* Transition Metal Halides

ZrF_4 exists in two polymorphic forms [13a, 42a]. A transition in MoF_6 has been reported from NMR studies [1a].

AgF undergoes a pressure transformation from NaCl to the CsCl structure [18b]. There is no thermal transition in AgCl or AgBr. AgI, which usually

exists in the B4 or wurtzite form (hexagonal $P6_3mc$; a=4.592 Å, c=7.510 Å) and in the B3 or sphalerite form 1 (low cubic, F43m, a=6.495 Å) both of which undergo a thermal transformation at 418 K to the B23 (high cubic) phase. The transformation is reversible and is associated with large ΔH as well as considerable thermal hysteresis, ΔT and volume change, ΔV; the transformation is likely to be of first order [39].

The existence of the low-cubic (sphalerite or B3-form) AgI was questioned by Majumdar and Roy [29]. Burley [12], however, reports the kinetics of the B3 → B4 transition in AgI by x-ray diffractometry at high temperature. The structure of the B23 (high-cubic) AgI has also been a subject of interest [22]. Statistical models have been employed to explain the type of one-dimensional polymorphism (polytypism) in AgI [44]. Accordingly, B3 and B4 are polytypes of AgI. CdI_2 is another example of polytypism.

AgBr enters into solid solution with AgI and the structures of the specific phases depend on the composition and temperature [3, 4]. The solid solutions of AgI and AgBr have the B3 and/or B4 structure up to ~10 percent AgBr, and with higher percent of AgBr the NaCl type of structure (B1 phase) is formed [16, 39]. About 25 percent of AgI seems to enter into solid solution with AgBr in the B1-phase. However, the literature data available on the solid solution limits and the range of stability of specific phases are widely different.

Pressure transitions of silver halides with B1-structure have been studied in detail, but there appears to be some uncertainty regarding the exact structures. The most commonly postulated high pressure structure is the CsCl type (B2) structure [2, 9], essentially because of its higher anion-cation coordination. X-ray studies have revealed this to be the case with ionic solids like rubidium and potassium halides. However, with more covalent solids this is not the case. It has been shown by x-ray studies that AgCl and AgBr under pressure transform to a cinnabar type of structure (B9) i.e., a tetragonal one [26, 47]. The different phases of AgI encountered in the high pressure transitions have different structures and ranges of stability [1, 5]. In the following table the high pressure phases of AgI are listed along with their structures and stability ranges.

Structure and Stability of Silver Iodide in the High Pressure Area

Designation	Structure	Lattice constants	Range of stability
I	B23, high cubic	a=5.074 Å at 443 K	Stable above ~ 419 K and up to ~ 80 kbar.
II	B4, wurtzite	a=4.591 Å, c=7.498 Å at 298 K.	Stable up to ~ 419 K and below ~ 2 kbar.
II′	B3, sphalerite	a=6.495 Å at 298 K	Stable below ~ 413 K and below ~ 2 kbar.
III	B1, NaCl type	a=6.07 at 298 K	Stable up to ~ 419 K and above 3–4 kbar.
IV	Orthorhombic	.....	Stable below ~ 320 K and between 2–4 kbar.
V	B2. CsCl type	.....	Stable above 95 kbar.

Lattice energies of silver halides have been calculated by Mayer [31], Huggins [23], Ladd and Lee [27], Sharma and Madan [45] and recently by Natarajan and Rao [39]. Most of these workers have employed the Born model. Lattice energy calculations have enabled a study of the relative stabilities of the various structures of silver halides and some of their solid solutions [39]. Born model has been employed to explain the pressure transitions in silver halides as well as the thermal transition in silver iodide [39]. Transition pressures have been theoretically determined by Jacob [24] employing the Born model.

Polytypism of Cadmium halides. Both $CdBr_2$ [8] and CdI_2 [18a] are known to exhibit polytypism [32, 35, 37, 44, 57a]. Single crystal x-ray studies on $CdBr_2$ grown from solution have shown that 6R is by far the most common polytype of $CdBr_2$. There are as many as 130 structures for the $CdBr_2$ polytypes [36]; 92 of these belong to the 6R type; sublimation of $CdBr_2$ also yields the 6R type.

Polytypism in CdI_2 has been found to be due to screw dislocations [32]. X-ray diffraction studies show the existence of many polytypes with different stacking sequences [31]. The entire "22 . . . 11" series of structures could be generated by spiral growth from single nonintegral screw dislocations in an "ideal" 4H structure [33, 34]. Other known structures not belonging to the "22 . . . 11" series could be generated by assuming the presence of two or more cooperative dislocations. These considerations suggest that polytypism is not expected in certain substances because of the nature of their ideal structures. A detailed discussion on polytypism is furnished by Verma and Krishna [57a].

Substances and measurement techniques	Data	Remarks	References
Zirconium tetrafluoride, ZrF_4 (Monoclinic, C_{2h}^6, $a = 11.69$ Å, $b = 9.87$ Å, $c = 7.64$ Å; $\beta = 126° 9'$ at 298 K)			
DTA and heat capacity	ZrF_4 undergoes a phase transition at ~ 680 K. The high temperature form is cubic (Fm3m) with $a = 7.88$ Å.	Heat capacity measurements in the range 5–307 K do not indicate any anomaly. DTA indicates a transition at ~ 680 K.	[13a, 42a, 58a].
Molybdenum hexafluoride, MoF_6			
NMR investigations of phase change in MoF_6 (temperature dependence of half width of the ^{19}F line).	Two jumps in half-line-width at ~ 263 K and at ~ 219 K are observed. The jump at 263 K is due to the phase transition in MoF_6 at ~ 263 K.	The spectra of the two modifications of MoF_6 are discussed in relation to the different types of Mo-F bonds and other symmetry considerations.	[1].
Silver Fluoride, AgF (Fm3m, $a = 4.932 \pm 0.003$ Å at 295 K)			
X-ray studies at different pressures.	Transforms to a new structure (probably B2 or CsCl) at ~ 26 kbar with $\Delta V = 1.64$ cm³ mol; $\Delta S \approx 4.2$–5.1 Joule/mole-deg.	The lattice parameter of the B2 phase (extrapolated to 1 bar) is 2.99 Å.	[18b].
Silver iodide, AgI (B3-AgI, $F\bar{4}3m$, $a = 6.495$ Å at 298 K; B4-AgI, $P6_3mc$, $a = 4.592$ Å, $c = 7.510$ Å at 298 K)			
Structure of various polymorphs of AgI by x-ray diffraction.	Three modifications of AgI are known; a low cubic-sphalerite (B3) phase stable upto 410 K, a hexagonal-wurtzite (B4 phase) which is formed when the AgI melt is cooled and a hot cubic (B23) form stable above 420 K. The hot cubic phase has a space centred lattice of I atoms, with $a = 5.04$ Å; Ag ions are distributed over the 30 largest gaps in the I structure.	The structure of B23-AgI was suggested to be tetragonal, but later work confirmed that the structure is an average between two structures of space groups Im3m and $I\bar{4}m2$. The structure of AgI precipitated from solution depends on the presence of excess of I^- or Ag^+ as well as the rate of precipitation.	[6, 7, 10,, 19, 21, 22, 28, 52, 60].
AgI polymorphism with DTA, X-ray etc.	Sphalerite to wurtzite transformation probably takes place over a wide temperature interval. The transition is associated with a $\Delta H_{tr} \sim 100$ cal · mol^{-1}. The energy of activation is ~ 10.3 ± 0.8 kcal · mol^{-1}. The low temperature phases of AgI transform to the B23 phase at ~ 420 K with a ΔH_{tr} of about 1600 cal · mol^{-1}.	The sphalerite-wurtzite transition is more likely to be an athermal higher order transition. Burley's [12] observation, however, suggests that the transition is a first-order one. Presence of iodine vapor seems to facilitate the B3 → B4 change at ~ 393 K. The T_t of B3/B4 → B23 transition also depends on the partial pressure of iodine. B3 → B4 transition is not seen by x-ray diffraction or DTA when small heating rates are employed. The B3/B4 → B23 transition is a well defined first order transition.	[11, 12, 22, 29, 30, 39, 43, 58, 59 54].

Substances and measurement techniques	Data	Remarks	References
B3/B4 → B23 transition investigated by emf method.	The emf of the cell, $Ag(s)\left\|AgI(s)\right\|\begin{matrix}CaCl_2\cdot 6H_2O\\AgI(C_1)\\PbI(C_2)\end{matrix}\left\|Pb(s)\right.$ was studied as a function of temperature. $T_t \sim 419.6$ K; $\Delta H_{tr} \sim 1270$ cal · mol^{-1}.		[14, 15].
Electrical Conductivity	The high ionic conductivity of the hot cubic (B23) phase above (420 K) of AgI is in accordance with a random orientation of silver ions in the lattice. E_a for conduction in B3 and B4 phases are ~0.2 and ~0.6 eV respectively.	The σ versus $1/T$ plots seem to suggest the transition of B3→ B4 to occur at ~410 K.	[20, 38, 39, 53].
X-ray and DTA study of the effect of AgBr on the AgI transition.	AgBr lowers the T_t to ~ 493 K at ~ 10% AgBr. This seems to be the solid solution limit in the low and high temperature phases. The specific phases of the solid solutions depend on the temperature as well as composition.	AgBr and AgI form an eutectic at ~ 68% AgBr with a eutectic temperature of ~ 613 K.	[3, 4, 16, 39, 51, 55].
Silver chloride, AgCl (Fm3m, a = 5.5491 Å at 299 K) *and Silver bromide* AgBr (Fm3m, a = 5.7745 Å at 299 K).			
X-ray diffraction of AgCl supported in amorphous boron vessel and subjected to quasi-hydrostatic pressures up to 150 kbar.	At ~ 25 kbar, ΔV is $\sim -0.9\, V_0$ where V_0 is the volume at 298 K and 1 atm. At higher pressures, the structure is shown to be that of Hg_2Cl_2; a = 3.92 Å, c = 9.03 Å and c/a = 2.30.	This is the first experimental evidence where a tetragonal structure is assigned to the AgCl high pressure phase.	[26].
X-ray diffraction	Both AgCl and AgBr do not transform to a B2 or CsCl-type structure. The high pressure phase in both the cases is of B9 type. For AgCl, a = 4.06 Å, c = 7.02 Å; c/a = 1.73. $\Delta V/V_0 \sim 8\%$ at the transition. For AgBr, a = 4.0 Å, c = 7.15 Å; c/a = 1.77.	The tetragonal structure is stabilized due to overlap of electron orbitals resulting in the formation of two highly covalent collinear bonds. The Hg_2Cl_2 type structure assigned to AgCl at high pressure is questioned.	[47].
Volumetric method	$P_T \sim 88$ kbar for AgCl; $P_T \sim 84$ kbar for AgBr.	The high pressure phases were considered to be of B2 structure.	[9].
Optical observation on single crystals.	$P_T \sim 90$ kbar for AgCl, $P_T \sim 86$ kbar for AgBr.		[2].
Pressure-temperature curves for AgCl and AgBr upto 60 kbar and 1073 K.	No change was observed in both the halides.	The pressure was not enough to detect the appearance of the high pressure phases.	[18].
Pressure transitions in AgI:			
High pressure transition in AgI investigated by x-rays.	At ~ 3 kbar the cell symmetry seem to belong to orthorhombic one. Moore and Kasper [37], however, consider the 3 kbar phase as tetragonal or pseudotetragonal.	Stability range of six polymorphs is indicated in a P–T diagram. The phase at 3 kbar is likely to be related to the NaCl structure, according to Moore and Kasper.	[1, 17, 37].
High pressure transition of AgI upto 60 kbar and x-ray investigation.	At ~60 kbar, AgI has the NaCl (B1) structure with a = 6.067 Å.		[40].

Substances and measurement techniques	Data	Remarks	References
High pressure transition in AgI up to ~ 120 kbar; examination by microscopic and x-ray diffraction techniques.	Microscopic examination indicates a transition at ~ 115 kbar. X-ray studies reveal that at ~ 97 kbar, the AgI transforms to a tetragonal structure with $a = 5.611$ Å, $c = 5.02$ Å and volume change is ~ 13%.	Electrical conductivity measurements suggest that the transition involves a significant change to more covalent bonding.	[2, 47].
High pressure transformation in AgI up to 100 kbar, and x-ray investigation.	As many as six polymorphs have been reported: B3, B4, B23, a 3 kbar phase, B1 structure and a sixth one.	The 3 kbar phase is yet to be identified exactly. There is a possible mutual transformation between B3, B4 and the '3 kbar' phases by a displacive mechanism rather than a reconstructive mechanism. This immediately suggests that B3, B4 and the 3 kbar phases are polytypes of AgI and should be very similar to each other energywise and structurewise.	[5].
High pressure transition in AgI by electrical conductivity measurements as a function of pressure up to 100 kbar.	Conductivity increases with pressure in the low pressure phase (stable upto 2.5 kbar) and then decreases in the two high pressure phases. The increase in the low pressure phase is in accordance with −ve thermal expansion. A reversal of the slope above 45 kbar in the (NaCl type) cubic phase is explained in terms of the formation of I_3^- ions.	Riggleman and Drickamer [42] however find a large increase in conductivity at ~ 97 kbar indicating a transformation.	[42, 46].
Cadmium fluoride, CdF_2			
X-ray study up to 160 kbar	CdF_2 transforms to the α-$PbCl_2$ structure reversibly around 60 kbar; $a = 3.368$ Å; $b = 5.690$ Å, $c = 6.730$ Å (at 120 kbar?).		[15a].
Cadmium bromide, $CdBr_2$ (hexagonal, $R\bar{3}m$, $a = 3.957$ Å, $c = 18.668$ Å)			
X-ray study of $CdBr_2$ polytypic structures.	An x-ray study of solution grown $CdBr_2$ crystals has revealed that 6R is by far the most common polytype. Other structures encountered include, 4H, 12H (or 12R), 4OH (or ~ 12OR) and some disordered structures.	Sublimation of $CdBr_2$ does not produce any polytype other than 6R. The relation between screw dislocations and polytypism is discussed.	[7, 36].
Cadmium iodide, CdI_2 (hexagonal, $P\bar{3}m1$, $a = 4.24$ Å, $c = 6.835$ Å)			
X-ray and interferometric studies of CdI_2 polytypism in relation to crystal growth.	A combined optical and x-ray diffraction study was made of polytypism of CdI_2 which grow by a dislocation mechanism. For the 2H and 4H structure types, a correlation between spiral step height and x-ray unit cell is found; with larger unit-cells no such correlation was observed. This is contrary to expectations on the basis of Frank's theory and can not be fully explained.	Thirteen new polytypes of CdI_2 are described. This number probably may be eighteen. In addition, several crystals resembling 2H and 4H types are also reported.	[56, 57].

Substances and measurement techniques	Data	Remarks	References
Investigation of the rhombohedral polytypes of CdI_2 and the transformation to hexagonal polytypes.	Two rhombohedral polytypes of CdI_2, 30R and 42R, grown from vapour phase are reported. Their complete structures are $(221212)_3$ and $(22221212)_3$ respectively.	Each of these polytypes occurs in syntactic coalescence with a hexagonal polytype having the same cell dimensions as the rhombohedral one showing that the lattice was transformed from hexagonal to rhombohedral or vice versa during crystal growth.	[13].
New polytypes of CdI_2	A 28 layered new polytype of CdI_2, designated as 28 Hc with unit cell dimensions, $a=4.24$ Å, $c=95.69$ Å has been described. The detailed atomic structure has been worked out and its zig zag sequence is found to be 2222222222221111. Another anomalous polytype of CdI_2 is 26 *Hc*.	The screw dislocation theory does not fully explain the growth of this polytype 28 Hc which is probably the largest polytype of CdI_2 known, with an atomic structure. 26 Hc also does not conform to the Frank screw dislocation theory. So the structure has been solved by a Fourier transform method as a special case using calculated and observed x-ray intensities distribution. Other anomalous polytypes of CdI_2 discussed, include 26 Hd, 50 Hc etc. Factors affecting the phenomenon of polytypism are enumerated.	[48, 49, 50].
X-ray investigation of polytypism as a higher order transformation.	Interaction energies for the known polytypic structures are calculated for CdI_2 on the basis of Schneer's theory of polytypism. Almost all polytypes are characterised by a maximum number of unlike interaction contacts.	This aspect was confirmed, experimentally by x-rays, which suggests a gradual transition from 3C to 2H structures.	[41].
X-ray study of the phenomenon of polytypism in CdI_2.	X-ray oscillation photographs of CdI_2 crystals reveal the existence of two different structures in parallel orientation on the same face of a crystal. This helped in understanding the frequent observation of the syntactic coalescence of two more polytypes in the same crystal as a phenomenon of epitaxial growth.	Prolonged microscopic observations have shown that 3-dimensional nuclei keep on forming at preferred sites during the growth of crystals. Subsequent x-ray investigation shows that it leads to the formation of a new polytypic structure of lower free-energy.	[25].

References

[1] Adams, L. H., and Davis, B. L., Am. J. Sci. **263**, 359 (1965).
[1a] Afanasév, M. L., Gabuda, S. P., Lundin, A. G., Opalovskii, A. A., and Khaldoyanidi, K. A., Izv. Sib. Otd. Akad. Nauk. SSSR, Ser. khim. Nauk. **4**, 18 (1968).
[2] van Valkenberg, Alvin, Jr., Rev. Sci, Instruments, **33**, 1462 (1962).
[3] Barth, T., and Lunde, G., Norsk. Geol. Tids. **8**, 293 (1925).
[4] Barth, T., and Lunde, G., Z. Physik. Chem. **122**, 293 (1926).
[5] Bassett, W. A., and Takahashi, T., Am. Mineralogist **50** (10), 1576 (1965).
[6] Berry, C. R., Phys. Rev. **161**, 848 (1967).
[7] Bijvoet, J. M., and Nieuwenkamp, W., Z. Krist. **86**, 466 (1933).
[8] Blocw, R., and Möller, H., Z. Physik. Chem. Vol A, **152**, 245 (1931).
[9] Bridgman, P. W., Proc. Am. Acad. Arts. Sci. **1**, 76 (1945).
[10] Burley G., J. Chem. Phys. **38**, 2807 (1963).
[11] Burley, G., Am. Mineralogist **48**, 1266 (1963).
[12] Burley, G., J. Phys. Chem. **68**, 1111 (1964).
[13] Chada, G. K., and Trigunayat, G. C., Acta. Cryst. **22**, 573 (1967).
[13a] Chrétien, A., and Gaudreau, B., Compt. rend. **246**, 2266 (1958).
[14] Cohen, E., and Joss, E. J., J. Am. Chem. Soc. **50**, 727 (1928).
[15] Cohen, E., and Joss, E. J., Verslag Akad. Wetenschappen Amsterdam, **36**, 980 (1927).
[15a] Dandekar, D. P., and Jamieson, J. C., personal communication (1971).
[16] de Cugnac, A., Chateau, H., and Pouradier, J., Compt. rend. Acad. Sci., Paris, Ser. C **14**, 264 (1967).
[17] Davis, B. L., and Adams, L. H., Science **146**, 519 (1964).
[18] Deaton, D. C., J. Appl. Phys. **36** (4), 1500 (1965).
[18a] Forty, A. J., Phil. Mag. **43**, 377 (1952).
[18b] Halleck, P. M., Jamieson, J. C., and Pistorius, C. W. F. T., personal communication (1971); J. Phys. Chem. Solids (in print).

[19] Helmholtz, L., J. Chem. Phys. **3**, 740 (1935).
[20] Hevesy, G. V., Z. Physik. Chem. **127**, 401 (1927).
[21] Hoshino, S., and Miyake, S., Science et. inds. phot. **25**, 154 (1954).
[22] Hoshino, S., J. Phys. Soc. Japan **12**, 315 (1957).
[23] Huggins, M. L., in Phase Transformations in Solids, Ed. R. Smoluchovski (John Wiley & Sons., Inc., New York, 1951).
[24] Jacobs, R. B., Phys. Rev. **54**, 468 (1938).
[25] Jain, R. K., and Trigunayat, G. C., J. Cryst. Growth **2** (5), 267 (1968).
[26] Jamieson, J. C., and Lawson, A. W., J. Appl. Phys. **33**, 776 (1962).
[27] Ladd, M. F. C., and Lee, W. H., J. Inorg. and Nuclear Chem. **11**, 264 (1959).
[28] Livitzkii, V., Ukrain. Khem. Zhur **10**, 283 (1935).
[29] Majumdar, A. J., and Roy, R., J. Phys. Chem. **63**, 1858 (1959).
[30] Manson, J. E., J. Phys. Chem. **60**, 806 (1956).
[31] Mayer, J. E., J. Chem. Phys. **1**, 327 (1933).
[32] Mitchell, R. S., Phil. Mag. **45**, 1093 (1954); ibid. **46**, 1141 (1955).
[33] Mitchell, R. S., Z. Krist. **108**, 296 (1956).
[34] Mitchell, R. S., Z. Krist. **108**, 341 (1957).
[35] Mitchell, R. S., Nature **182**, 337 (1958).
[36] Mitchell, R. S., Z. Krist. **117**, 309 (1962).
[37] Moore, M. J., and Kasper, J. S., J. Chem. Phys. **48**, 2446 (1968).
[38] Mrgudich, J. N., J. Electrochem. Soc. **107**, 475 (1960).
[39] Natarajan, M., and Rao, C. N. R., J. Chem. Soc. (London), **A**, 3087 (1970).
[40] Piermarini, G. J., and Weir, C. E., J. Res. Nat. Bur. Stand. (U.S.) **A66**, (Phys. and Chem.), No. 4, 325 (1962).
[41] Rai, K. N., and Krishna, P., Indian J. Pure and Appl. Phys. **6**, 118 (1968).
[42] Riggleman, B. M., and Drickamer, H. G., J. Chem. Phys. **38**, 2721 (1963).
[42a] Robbins, G. D., Thoma, R. E., and Insley, H., J. Inorg. Nucl. Chem. **27**, 559 (1965).
[43] Schneer, C. J., and Whiting, W., Jr., Am. Mineralogist **48**, 737 (1963).
[44] Schneer, C. J., Acta. Cryst. **8**, 279 (1955).
[45] Sharma, M. N., and Madan, M. P., Indian J. Physics **38**, 305 (1964).
[46] Shock R. N., and Katz, S., J. Chem. Phys. **48**, 2094 (1968).
[47] Shock, R. N., and Jamieson, J. C., J. Phys. Chem. Solids **30**, 1527 (1969).
[48] Srivastava, O. N., and Verma, A. R., Proc. Nucl. Phys. Solid State Symp., Chandigarh, India, Part B, 362 (1964).
[49] Srivastava, O. N., and Verma, A. R., Acta. Cryst. **17**, 260 (1964).
[50] Srivastava, O. N., and Verma, A. R., Acta. Cryst. **19**, 56 (1965).
[51] Stasiw O., and Teltow, J., Z. anorg. Chem. **259**, 143 (1949).
[52] Strock, L. W., Z. physik. chem. **B25**, 441 (1934).
[53] Takahashi, T., Katusmi, K., and Osamu, Y., J. Electrochem. Soc., **116**, 357 (1969).
[54] Tamman, G., Z. Physik. chem. **75**, 733 (through Chemical Abstracts, **5**, 1219).
[55] Tamman, G., Z. anorg. chem. **91**, 263 (1915).
[56] Trigunayat, G. C., and Verma, A. R., Acta. Cryst. **15**, 499 (1962).
[57] Verma, A. R., J. Sci. Ind. Res. **25**, 487 (1966).
[57a] Verma, A. R., and Krishna, P., Polymorphism and Polytypism in Crystals (John Wiley, 1966).
[58] Weiss, K., and Vermaas, P. A., Z. physik. chem. **44**, 372 (1965).
[58a] Westrum, E. F., Jr., J. Chem. Eng. Data **10**, 140 (1965).
[59] Winkler, H. G. F., Z. anorg. u. allgem. chem. **276**, 169 (1954).
[60] Yamada, K., Bull. Soc. Sci. Phot. Japan No. **11**, 1 (1961).

10. 5*d* Transition Metal Halides

$OsCl_4$ is known to exist in two polymorphic forms [15]. Transitions in mercury halides are also known. Both mercuric chloride and mercuric bromide are orthorhombic at room temperature. No detailed phase transformation data are available for these two halides. Some information regarding the isomorphic relations of these halides as well as their mixed salts are available [11, 12].

Red mercuric iodide is tetragonal and is the stable phase at room temperature. The change of red HgI_2 to the orthorhombic yellow variety takes place reversibly at ~403 K. The effect of state of aggregation [1], heating rate [3, 5] and the presence of other halides [10] on the T_t have been studied. The theory of dynamic allotropy has been found to be applicable to the HgI_2 transition [5]. The kinetics of the tetragonal-orthorhombic transition in HgI_2 has been studied by Baram [2] and others [3, 6]. The mechanism of the transition [14] has been discussed by Johansson [7], from considerations of the structures of the two modifications. The HgI_2 transition has been considered as an example of a topochemical reaction which takes place in the inner or outer fields of force of the crystalline matter [8, 9]. The high temperature yellow HgI_2 could be stabilized on Al_2O_3 base provided the sample is free from moisture [17]. Recently, the HgI_2 transition has been studied with low frequency laser excited Raman spectroscopy [13]. A third variety of HgI_2 has been reported [16]. A pressure transition in HgI_2 was reported by Bridgman [4].

Substances and measurement techniques	Data	Remarks	References
Osmium tetrachloride. $OsCl_4$ (cubic. $a=9.5$ Å at 298 K)			
X-ray and magnetic measurements	A solution of OsO_4 when refluxed with $SOCl_4$ yields the cubic form. This is a dark-brown solid. It belongs to the space-group $O^6-P4_3[32]$ or $O^7-P4_1[32]$. OsO_4 and CCl_4 when reacted in a sealed tube at ~ 743 K, yield the high temperature orthorhombic form ($a=12.08$ Å, $b=11.96$ Å and $c=11.68$ Å).	Both the low and high temperature forms are paramagnetic and display magnetic susceptibilities as a result of strong spin-orbit coupling: the high temperature form exhibits the temperature dependent magnetic susceptibility.	[15].
Mercuric iodide. HgI_2 (Tetragonal, $a=4.39$ Å, $c=12.38$ Å at 296 K).			
Factors affecting the T_t of HgI_2	A freshly prepared sol. of HgI_2 transforms at a lower temperature. The T_t increases as precipitation continues. T_t is also affected by other halides such as $HgCl_2$, HgBr etc.	The yellow sol. when dried is covered with a red layer which disappears slowly.	[1, 10].
Dilatometry and kinetics	The transition from red to yellow variety takes place at ~ 400 K. The dilatometric studies indicate that the transition is autocatalytic in both the directions. Quenching experiments indicate that the theory of dynamic allotropy is applicable to HgI_2 transition. $\Delta V \sim 0.0028$ cm^3 g^{-1}.	Transition rates in the range 400–406 K are almost the same in the presence of air, CO_2 or nitrogen. However, presence of hydrogen or oxygen has a definite effect on the speed of the conversion of yellow to red form. An inconclusive evidence for a white modification of HgI_2 is also mentioned.	[2, 3, 5, 6, 8, 9].
Low frequency laser Raman spectra.	Raman bands for red HgI_2 are at 17.5, 29 and 114 cm^{-1}: in addition, weaker bands are seen at 46, 142, and 246 cm^{-1}. For yellow HgI_2, stronger bands are at 37, 41, and 138 cm^{-1}: a weaker band is seen at ~ 278 cm^{-1}.	Marked changes in the spectra were attributed to changes in crystal structure.	[13].

References

[1] Balarev, D., Chemie **47**, 27 (1952).
[2] Baram, O. M., ukrain. khim. Zhur. **22**, 137 (1956).
[3] Benton, A. F., and Cool, R. D., J. Phys. Chem. **35**, 1762 (1931).
[4] Bridgman, P. W., Proc. Am. Acad. Arts Sci. **51**, 55 (1915).
[5] Damiens, A., compt. rend. **177**, 816 (1923).
[6] Eade, D. G., and Hartshorne, N. H., J. Chem. Soc. 1636 (1938).
[7] Johansson, G., Arkiv Kemi **8**, 153 (1955).
[8] Kohlscüutter, H. W., kolloid chem. Beihefte **24**, 319 (1927).
[9] Kohlscüutter, V., kolloid-Z **42**, 254 (1927).
[10] Losana, L., Gazz. Chim. ital. **56**, 301 (1926).
[11] Luczizkii, W., Mem. Soc. Nat. Kiew. **20**, 191 (through Chemical Abstracts. **1**, 2849[2]).
[12] Luczizkii, V. I., Z. Krist. Min. **46**, 297 (through Chemical Abstracts, **6**, 57[9]).
[13] Melveger, A. J., Khanna, R. K., Guscott, B. R., and Lippincott, E. R., Inorg. Chem. **7**, 1630 (1968).
[14] Newkirk, J. B., Acta. Met. **4**, 316 (1956).
[15] Paul, M., Z. Naturforsch **24**, 200 (1969).
[16] Seiskind, M., Michel, P., and Grun, J. B., J. Chim. Phys. **56**, 858 (1959).
[17] Zeitlin, H., and Goya, H., Nature **183**, 1041 (1959).

11. Rare-Earth Trifluorides

The crystal structures of some of the rare-earth fluorides like SmF_3, EuF_3, HoF_3, and TmF_3 depend on the method of preparation [2]. The fluorides can thus exist in a hexagonal structure or an orthorhombic one. YF_3 is orthorhombic at room temperature. A cubic modification of YF_3 reported by

Nowachi [1] has not been reproducible. The preparation of the various fluorides and their crystal dimensions have been reported by Zalkin and Templeton [2].

The hexagonal trifluoride seems to be the only stable form for elements from lanthanum to neodymium. It is likely that it can be produced under proper conditions for the rest of the rare-earth elements and also yttrium, although this has not been achieved in several cases. The data on LnF_3 structures are best understood if only the hexagonal form is stable at elevated temperatures even though it may be precipitated from solution under certain conditions because of greater ease of crystal nucleation and growth.

References

[1] Nowacki, W., Z. krist. **100**, 242 (1938).

[2] Zalkin, A., and Templeton, D. H., J. Am. Chem. Soc. **75**, 2453 (1953).

12. Inert Gas Halides

Xenon fluorides (XeF_2, XeF_4, XeF_6, etc.) have been well characterized in the literature. Two forms of XeF_4 have been reported from x-ray studies. XeF_6 has been found to exhibit interesting thermal properties [3]. Heat capacity measurements have indicated the existence of two phase transitions [3], in the range 200–300 K. The crystal structures of two XeF_6 phases have been reported [1].

Inert Gas Halides

Substances and measurement techniques	Data	Remarks	References
Xenon tetrafluoride, XeF_4			
X-ray studies	Two monoclinic forms I and II are reported for XeF_4. Form I belongs to $P2_1/C$ space group with $a=6.64\pm0.01$ Å, $b=7.33\pm0.01$ Å, $c=6.40\pm0.01$ Å; $\beta=92°40'\pm5'$. $\rho=4.42$ g cm^{-3}. Form II belongs to $P2_1/n$ space group with $a=5.03$ Å, $b=5.92$ Å, $c=5.79$ Å; $\beta=99°27'$. $\rho=4.04$ g cm^{-3}.	The greater density of form I suggests that this is the lower temperature polymorph of XeF_4.	[2, 4, 5].
Xenon hexafluoride, XeF_6			
X-ray and neutron diffraction	Single crystals of XeF_6 were grown by sublimation in a thermal gradient near room temperature. The crystal structure belongs to $P2_1/m$ or $P2_1$ space group (monoclinic) with $a=9.33\pm0.03$ Å, $b=10.36\pm0.03$ Å, $c=8.95\pm0.03$ Å; $\beta=91.9\pm0.2°$. A second modification of XeF_6, belongs to $F\bar{4}3c$ or $Fm3c$, with $a=25.34\pm0.05$ Å. This (FCC) XeF_6 transforms to the third form around 295 K with a hysteresis of $\sim 8°$.	The crystal structure of the form III is still to be worked out.	[1].
Calorimetry	Very large specific heat anomalies are observed in the regions 241–261 K and 288–297 K.	The anomalies are probably due to slow phase transitions.	[3].

References

[1] Agron, P. A., Johnson, C. K., and Levy, H. A., Inorg. Nucl. Chem. Letters **1**, 145 (1965).

[2] Burns, J. H., J. Phys. Chem. **67**, 536 (1963).

[3] Malm, J. G., Schreiner, F., and Osborne, D. W., Inorg. Nucl. Chem. Letters **1**, 97 (1965).

[4] Siegel, S., and Gerbert, E., J. Am. Chem. Soc. **85**, 240 (1963).

[5] Templeton, D. H., Zalkin, A., Forrester, J. D., and Williamson, S. M., J. Am. Chem. Soc. **85**, 242 (1963).

13. Halogens

Substances and measurement techniques	Data	Remarks	References
Fluorine			
Heat capacity as a function of temperature	$T_t \sim 45.55 \pm 0.02$ K ΔH_{tr}. 173.9 ± 0.004 cal·mol^{-1} Entropy of fluorine at 85.02 K $= 39.58 \pm 0.16$ e.u.	The transition is indicated by an anomaly in $C_p(T)$ curves. The transition had been suspected by Murphy and Rubin [3] from an analysis of the heat capacity data of Kanda [2].	[1].
Bromine			
P–T behavior of single crystals up to 273 K.	A new solid phase at high pressures ($\sim$35 kbar) and at $\sim$273 K is reported with the space group Cmca (orthorhombic) $a = 4.79$ Å, $b = 6.75$ Å and $c = 8.63$ Å.		[4].

References

[1] Hu, J. H., White, D., and Johnston, H. L., J. Am. Chem. Soc. **75**, 5642 (1953).

[2] Kanda, E., Bull. Chem. Soc. Japan, **12**, 473 (1937).

[3] Murphy, G. M., and Rubin, E., J. Chem. Phys. **20**, 1179 (1952).

[4] Wier, C. E., Piermarini, G. J., and Block, S., J. Chem. Phys. **50**, 2089 (1969).

Announcement of New Publications on Standard Reference Data

Superintendent of Documents,
Government Printing Office,
Washington, D.C. 20402

Dear Sir:

Please add my name to the announcement list of new publications to be issued in the series: National Standard Reference Data Series—National Bureau of Standards.

Name_____

Company_____

Address_____

City_____ State_____ Zip Code_____

(Notification Key N337)

Publications in the National Standard Reference Data Series
National Bureau of Standards

You may use this listing as your order form by checking the proper box of the publication(s) you desire or by providing the full identification of the publication you wish to purchase. The full letter symbols with each publication number and full title of the publication and author must be given in your order, e.g. NSRDS—NBS—21, **Kinetic Data on Gas Phase Unimolecular Reactions,** by S. W. Benson and H. E. O'Neal.

Pay for publications by check, money order, or Superintendent of Documents coupons or deposit account. Make checks and money orders payable to Superintendent of Documents. Foreign remittances should be made either by international money order or draft on an American bank. Postage stamps are not acceptable.

No charge is made for postage to destinations in the United States and possessions, Canada, Mexico, and certain Central and South American countries. To other countries, payments for documents must cover postage. Therefore, one-fourth of the price of the publication should be added for postage.

Send your order together with remittance to Superintendent of Documents, Government Printing Office, Washington, D.C. 20402.

☐ NSRDS-NBS 1, **National Standard Reference Data System—Plan of Operation,** by E. L. Brady and M. B. Wallenstein, 1964 (15 cents), SD Catalog No. C13.48:1.

☐ NSRDS-NBS 2, **Thermal Properties of Aqueous Uni-univalent Electrolytes,** by V. B. Parker, 1965 (45 cents), SD Catalog No. C13.48:2.

☐ NSRDS-NBS 3, Sec. 1, **Selected Tables of Atomic Spectra, Atomic Energy Levels and Multiplet Tables, Si II, Si III, Si IV,** by C. E. Moore, 1965 (35 cents), SD Catalog No. C13.48:3/Sec.1.

☐ NSRDS-NBS 3, Sec. 2, **Selected Tables of Atomic Spectra, Atomic Energy Levels and Multiplet Tables, Si I,** by C. E. Moore, 1967 (20 cents), SD Catalog No. C13.48:3/Sec.2.

☐ NSRDS-NBS 3, Sec. 3, **Selected Tables of Atomic Spectra, Atomic Energy Levels and Multiplet Tables, C I, C II, C III, C IV, C V, C VI,** by C. E. Moore, 1970 ($1), SD Catalog No. C13.48:3/Sec.3.

☐ NSRDS-NBS 3, Sec. 4, **Selected Tables of Atomic Spectra, Atomic Energy Levels and Multiplet Tables, N IV, N V, N VI, N VII,** by C. E. Moore, 1971 (55 cents), SD Catalog No. C13.48:3/Sec.4.

☐ NSRDS–NBS 3, Sec. 6, **Selected Tables of Atomic Spectra, Atomic Energy Levels and Multiplet Tables, HI , D, T,** by C. E. Moore, 1971 (In press), SD Catalog No. C13.48:3/Sec. 6.

☐ NSRDS-NBS 4, **Atomic Transition Probabilities, Vol. I, Hydrogen Through Neon,** by W. L. Wiese, M. W. Smith, and B. M. Glennon, 1966 ($2.50), SD Catalog No. C13.48:4/Vol. I.

☐ NSRDS-NBS 5, **The Band Spectrum of Carbon Monoxide,** by P. H. Krupenie, 1966 (70 cents), SD Catalog No. C13.48:5.

☐ NSRDS-NBS 6, **Tables of Molecular Vibrational Frequencies, Part 1,** by T. Shimanouchi, 1967 (40 cents), SD Catalog No. C13.48:6/Pt.1. Superseded by NSRDS-NBS 39.

☐ NSRDS-NBS 7, **High Temperature Properties and Decomposition of Inorganic Salts, Part 1. Sulfates,** by K. H. Stern and E. L. Weise, 1966 (35 cents), SD Catalog No. C13.48:7/Pt.1.

☐ NSRDS-NBS 8, **Thermal Conductivity of Selected Materials,** by R. W. Powell, C. Y. Ho,

and P. E. Liley, 1966 ($3). PB189698*

☐ NSRDS-NBS 9, **Tables of Bimolecular Gas Reactions,** by A. F. Trotman-Dickenson and G. S. Milne, 1967 ($2), SD Catalog No. C13.48:9.

☐ NSRDS-NBS 10, **Selected Values of Electric Dipole Moments for Molecules in the Gas Phase,** by R. D. Nelson, Jr., D. R. Lide, Jr., and A. A. Maryott, 1967 (40 cents), SD Catalog No. C13.48:10.

☐ NSRDS-NBS 11, **Tables of Molecular Vibrational Frequencies, Part 2,** by T. Shimanouchi, 1967 (30 cents), SD Catalog No. C13.48:11/Pt.2. Superseded by NSRDS-NBS 39.

☐ NSRDS-NBS 12, **Tables for the Rigid Asymmetric Rotor: Transformation Coefficients from Symmetric to Asymmetric Bases and Expectation Values of P_z^2, P_z^4 and P_z^6,** by R. H. Schwendeman, 1968 (60 cents), SD Catalog No. C13.48:12.

☐ NSRDS-NBS 13, **Hydrogenation of Ethylene on Metallic Catalysts,** by J. Horiuti and K. Miyahara, 1968 ($1), SD Catalog No. C13.48:13.

☐ NSRDS-NBS 14, **X-Ray Wavelengths and X-Ray Atomic Energy Levels,** by J. A. Bearden, 1967 (40 cents), SD Catalog No. C13.48:14.

☐ NSRDS-NBS 15, **Molten Salts: Vol. 1, Electrical Conductance, Density, and Viscosity Data,** by G. J. Janz, F. W. Dampier, G. R. Lakshminarayanan, P. K. Lorenz, and R. P. T. Tomkins, 1968 ($3), SD Catalog No. C13.48:15/Vol.1.

☐ NSRDS-NBS 16, **Thermal Conductivity of Selected Materials, Part 2,** by C. Y. Ho, R. W. Powell, and P. E. Liley, 1968 ($2), SD Catalog No. C13.48:16/Pt.2.

☐ NSRDS-NBS 17, **Tables of Molecular Vibrational Frequencies, Part 3,** by T. Shimanouchi, 1968 (30 cents), SD Catalog No. C13.48:17/Pt.3. Superseded by NSRDS-NBS 39.

☐ NSRDS-NBS 18, **Critical Analysis of the Heat-Capacity Data of the Literature and Evaluation of Thermodynamic Properties of Copper, Silver, and Gold from 0 to 300 K,** by G. T. Furukawa, W. G. Saba, and M. L. Reilly, 1968 (40 cents), SD Catalog No. C13.48:18.

☐ NSRDS-NBS 19, **Thermodynamic Properties of Ammonia as an Ideal Gas,** by L. Haar, 1968 (20 cents), SD Catalog No. C13.48:19.

☐ NSRDS-NBS 20, **Gas Phase Reaction Kinetics of Neutral Oxygen Species,** by H. S. Johnston, 1968 (45 cents), SD Catalog No. C13.48:20.

☐ NSRDS-NBS 21, **Kinetic Data on Gas Phase Unimolecular Reactions,** by S. W. Benson and H. E. O'Neal, 1970 ($7), SD Catalog No. C13.48:21.

☐ NSRDS-NBS 22, **Atomic Transition Probabilities, Vol. II, Sodium Through Calcium, A Critical Data Compilation,** by W. L. Wiese, M. W. Smith, and B. M. Miles, 1969 ($4.50), SD Catalog No. C13.48:22/Vol.II.

☐ NSRDS-NBS 23, **Partial Grotrian Diagrams of Astrophysical Interest,** by C. E. Moore and P. W. Merrill, 1968 (55 cents), SD Catalog No. C13.48:23.

☐ NSRDS-NBS 24, **Theoretical Mean Activity Coefficients of Strong Electrolytes in Aqueous Solutions from 0 to 100 °C,** by Walter J. Hamer, 1968 ($4.25), SD Catalog No. C13.48:24.

☐ NSRDS-NBS 25, **Electron Impact Excitation of Atoms,** by B. L. Moiseiwitsch and S. J. Smith, 1968 ($2), SD Catalog No. C13.48:25.

☐ NSRDS-NBS 26, **Ionization Potentials, Appearance Potentials, and Heats of Formation of Gaseous Positive Ions,** by J. L. Franklin, J. G. Dillard, H. M. Rosenstock, J. T. Herron, K. Draxl, and F. H. Field, 1969 ($4), SD Catalog No. C13.48:26.

☐ NSRDS-NBS 27, **Thermodynamic Properties of Argon from the Triple Point to 300 K at Pressures to 1000 Atmospheres,** by A. L. Gosman, R. D. McCarty, and J. G. Hust, 1969 ($1.25), SD Catalog No. C13.48:27.

☐ NSRDS-NBS 28, **Molten Salts: Vol. 2, Section 1. Electrochemistry of Molten Salts: Gibbs Free Energies and Excess Free Energies from Equilibrium-Type Cells,** by G. J. Janz and C. G. M. Dijkhuis; **Section 2. Surface Tension Data,** by G. J. Janz, G. R. Lakshminarayanan, R. P. T. Tomkins, and J. Wong, 1969 ($2.75), SD Catalog No. C13.48:28/Vol.2.

☐ NSRDS-NBS 29, **Photon Cross Sections, Attenuation Coefficients, and Energy Absorption Coefficients from 10 keV to 100 GeV,** by J. H. Hubbell, 1969 (75 cents), SD Catalog No. C13.48:29.

☐ NSRDS-NBS 30, **High Temperature Properties and Decomposition of Inorganic Salts, Part 2. Carbonates,** by K. H. Stern and E. L. Weise, 1969 (45 cents), SD Catalog No. C13.48:30/Pt.2.

☐ NSRDS-NBS 31, **Bond Dissociation Energies**

---

*Available from National Technical Information Service, Springfield, Virginia 22151.

in Simple Molecules, by B. deB. Darwent, 1970 (55 cents), SD Catalog No. C13.48:31.

☐ NSRDS-NBS 32, **Phase Behavior in Binary and Multicomponent Systems at Elevated Pressures: *n*-Pentane and Methane-*n*-Pentane,** by V. M. Berry and B. H. Sage, 1970 (70 cents), SD Catalog No. C13.48:32.

☐ NSRDS-NBS 33, **Electrolytic Conductance and the Conductances of the Halogen Acids in Water,** by W. J. Hamer and H. J. DeWane, 1970 (50 cents), SD Catalog No. C13.48:33.

☐ NSRDS-NBS 34, **Ionization Potentials and Ionization Limits Derived from the Analyses of Optical Spectra,** by C. E. Moore, 1970 (75 cents), SD Catalog No. C13.48:34.

☐ NSRDS-NBS 35, **Atomic Energy Levels as Derived from the Analyses of Optical Spectra, Vol. I, ^{1}H to ^{23}V; Vol. II, ^{24}Cr to ^{41}Nb; Vol. III, ^{42}Mo to ^{57}La, ^{72}Hf to ^{89}Ac,** by C. E. Moore, 1971 (Vol. I, $5; Vol. II, $4.25; Vol. III, $4.50), SD Catalog No. C13.48:35/Vols. I, II, and III.

☐ NSRDS-NBS 36, **Critical Micelle Concentrations of Aqueous Surfactant Systems,** by P. Mukerjee and K. J. Mysels, 1971 ($3.75), SD Catalog No. C13.48:36.

☐ NSRDS-NBS 37, **JANAF Thermochemical Tables, 2d Edition,** by D. R. Stull, H. Prophet, et al., 1971 ($9.75), SD Catalog No. C13.48:37.

☐ NSRDS-NBS 38, **Critical Review of Ultraviolet Photoabsorption Cross Sections for Molecules of Astrophysical and Aeronomic Interest,** by R. D. Hudson, 1971 ($1), SD Catalog No. C13.48:38.

☐ NSRDS–NBS 39, **Tables of Molecular Vibrational Frequencies, Consolidated Tables,** by T. Shimanouchi, 1972 (In press), SD Catalog No. C13.48:39.

☐ NSRDS–NBS 40, **A Multiplet Table of Astrophysical Interest** (Reprint of 1945 Edition), by C. E. Moore, 1972 ($2), SD Catalog No. C13.48:40.

☐ NSRDS–NBS 41, **Crystal Structure Transformations in Binary Halides,** by C. N. R. Rao, 1972 (In press), SD Catalog No. C13.48:41.

☐ NSRDS–NBS 42, **Selected Specific Rates of Reactions of the Solvated Electron in Alcohols,** by E. Watson, Jr., and S. Roy, 1972 (In press), SD Catalog No. C13.48:42.

☐ NSRDS–NBS 43, **Selected Specific Rates of Reactions of Transients from Water in Aqueous Solution,** by M. Anbar, M. Bambenek, and A. B. Ross, 1972 (In press), SD Catalog No. C13.48:43.

☐ NSRDS–NBS 44, **The Radiation Chemistry of Gaseous Ammonia,** by D. B. Peterson, 1972 (In press), SD Catalog No. C13.48:44.

FORM NBS-114A (1-71)

U.S. DEPT. OF COMM. BIBLIOGRAPHIC DATA SHEET	1. PUBLICATION OR REPORT NO. NBS-NSRDS-41	2. Gov't Accession No.	3. Recipient's Accession No.

4. TITLE AND SUBTITLE

Crystal Structure Transformations in Binary Halides

5. Publication Date: July 1972

6. Performing Organization Code

7. AUTHOR(S)
C.N.R. Rao and M. Natarajan

8. Performing Organization

9. PERFORMING ORGANIZATION NAME AND ADDRESS

NATIONAL BUREAU OF STANDARDS
DEPARTMENT OF COMMERCE
WASHINGTON, D.C. 20234

10. Project/Task/Work Unit No.

11. Contract/Grant No.

12. Sponsoring Organization Name and Address

Same as No. 9

13. Type of Report & Period Covered
N/A

14. Sponsoring Agency Code

15. SUPPLEMENTARY NOTES

16. ABSTRACT (A 200-word or less factual summary of most significant information. If document includes a significant bibliography or literature survey, mention it here.)

A critical survey of the data describing crystal structure transformations in binary halides is compiled. Data on thermodynamic, crystallographic, spectroscopic and electronic properties are given for each transformation. Experimental techniques used to obtain the data are named and comments on the data are included in the tables. The literature is surveyed up to 1970. References have been selected on the basis of their pertinence to the data which are cited and do not represent all the available literature.

17. KEY WORDS (Alphabetical order, separated by semicolons)

Binary halides; Crystal structure transformation; Electronic data; Phase transformation; Spectroscopic data; Thermodynamic data; X-ray diffraction data.

18. AVAILABILITY STATEMENT

[X] UNLIMITED.

[ ] FOR OFFICIAL DISTRIBUTION. DO NOT RELEASE TO NTIS.

19. SECURITY CLASS (THIS REPORT): UNCLASSIFIED

21. NO. OF PAGES: 53

20. SECURITY CLASS (THIS PAGE): UNCLASSIFIED

22. Price: 55 Cents

USCOMM-DC 66244-P7

U. S. GOVERNMENT PRINTING OFFICE - 1972 O - 456-089

NBS TECHNICAL PUBLICATIONS

PERIODICALS

JOURNAL OF RESEARCH reports National Bureau of Standards research and development in physics, mathematics, and chemistry. Comprehensive scientific papers give complete details of the work, including laboratory data, experimental procedures, and theoretical and mathematical analyses. Illustrated with photographs, drawings, and charts. Includes listings of other NBS papers as issued.

Published in two sections, available separately:

- **Physics and Chemistry**

Papers of interest primarily to scientists working in these fields. This section covers a broad range of physical and chemical research, with major emphasis on standards of physical measurement, fundamental constants, and properties of matter. Issued six times a year. Annual subscription: Domestic, $9.50; $2.25 additional for foreign mailing.

- **Mathematical Sciences**

Studies and compilations designed mainly for the mathematician and theoretical physicist. Topics in mathematical statistics, theory of experiment design, numerical analysis, theoretical physics and chemistry, logical design and programming of computers and computer systems. Short numerical tables. Issued quarterly. Annual subscription: Domestic, $5.00; $1.25 additional for foreign mailing.

TECHNICAL NEWS BULLETIN

The best single source of information concerning the Bureau's measurement, research, developmental, cooperative, and publication activities, this monthly publication is designed for the industry-oriented individual whose daily work involves intimate contact with science and technology—*for engineers, chemists, physicists, research managers, product-development managers, and company executives.* Includes listing of all NBS papers as issued. Annual subscription: Domestic, $3.00; $1.00 additional for foreign mailing.

Bibliographic Subscription Services

The following current-awareness and literature-survey bibliographies are issued periodically by the Bureau: Cryogenic Data Center Current Awareness Service (weekly), Liquefied Natural Gas (quarterly), Superconducting Devices and Materials (quarterly), and Electromagnetic Metrology Current Awareness Service (monthly). Available only from NBS Boulder Laboratories. Ordering and cost information may be obtained from the Program Information Office, National Bureau of Standards, Boulder, Colorado 80302.

NONPERIODICALS

Applied Mathematics Series. Mathematical tables, manuals, and studies.

Building Science Series. Research results, test methods, and performance criteria of building materials, components, systems, and structures.

Handbooks. Recommended codes of engineering and industrial practice (including safety codes) developed in cooperation with interested industries, professional organizations, and regulatory bodies.

Special Publications. Proceedings of NBS conferences, bibliographies, annual reports, wall charts, pamphlets, etc.

Monographs. Major contributions to the technical literature on various subjects related to the Bureau's scientific and technical activities.

National Standard Reference Data Series. NSRDS provides quantitative data on the physical and chemical properties of materials, compiled from the world's literature and critically evaluated.

Product Standards. Provide requirements for sizes, types, quality, and methods for testing various industrial products. These standards are developed cooperatively with interested Government and industry groups and provide the basis for common understanding of product characteristics for both buyers and sellers. Their use is voluntary.

Technical Notes. This series consists of communications and reports (covering both other-agency and NBS-sponsored work) of limited or transitory interest.

Federal Information Processing Standards Publications. This series is the official publication within the Federal Government for information on standards adopted and promulgated under the Public Law 89–306, and Bureau of the Budget Circular A–86 entitled, Standardization of Data Elements and Codes in Data Systems.

Consumer Information Series. Practical information, based on NBS research and experience, covering areas of interest to the consumer. Easily understandable language and illustrations provide useful background knowledge for shopping in today's technological marketplace.

CATALOGS OF NBS PUBLICATIONS

NBS Special Publication 305, Publications of the NBS. 1966-1967. When ordering, include Catalog No. C13.10:305. Price $2.00; 50 cents additional for foreign mailing.

NBS Special Publication 305, Supplement 1, Publications of the NBS, 1968-1969. When ordering, include Catalog No. C13.10:305/Suppl. 1. Price $4.50; $1.25 additional for foreign mailing.

NBS Special Publication 305, Supplement 2, Publications of the NBS, 1970. When ordering, include Catalog No. C13.10:305/Suppl. 2. Price $3.25; 85 cents additional for foreign mailing.

Order NBS publications (except Bibliographic Subscription Services) from: Superintendent of Documents, Government Printing Office, Washington, D.C. 20402.

U.S. DEPARTMENT OF COMMERCE
National Bureau of Standards
Washington, D.C. 20234

OFFICIAL BUSINESS

Penalty for Private Use, $300

POSTAGE AND FEES PAID
U.S. DEPARTMENT OF COMMERCE
215